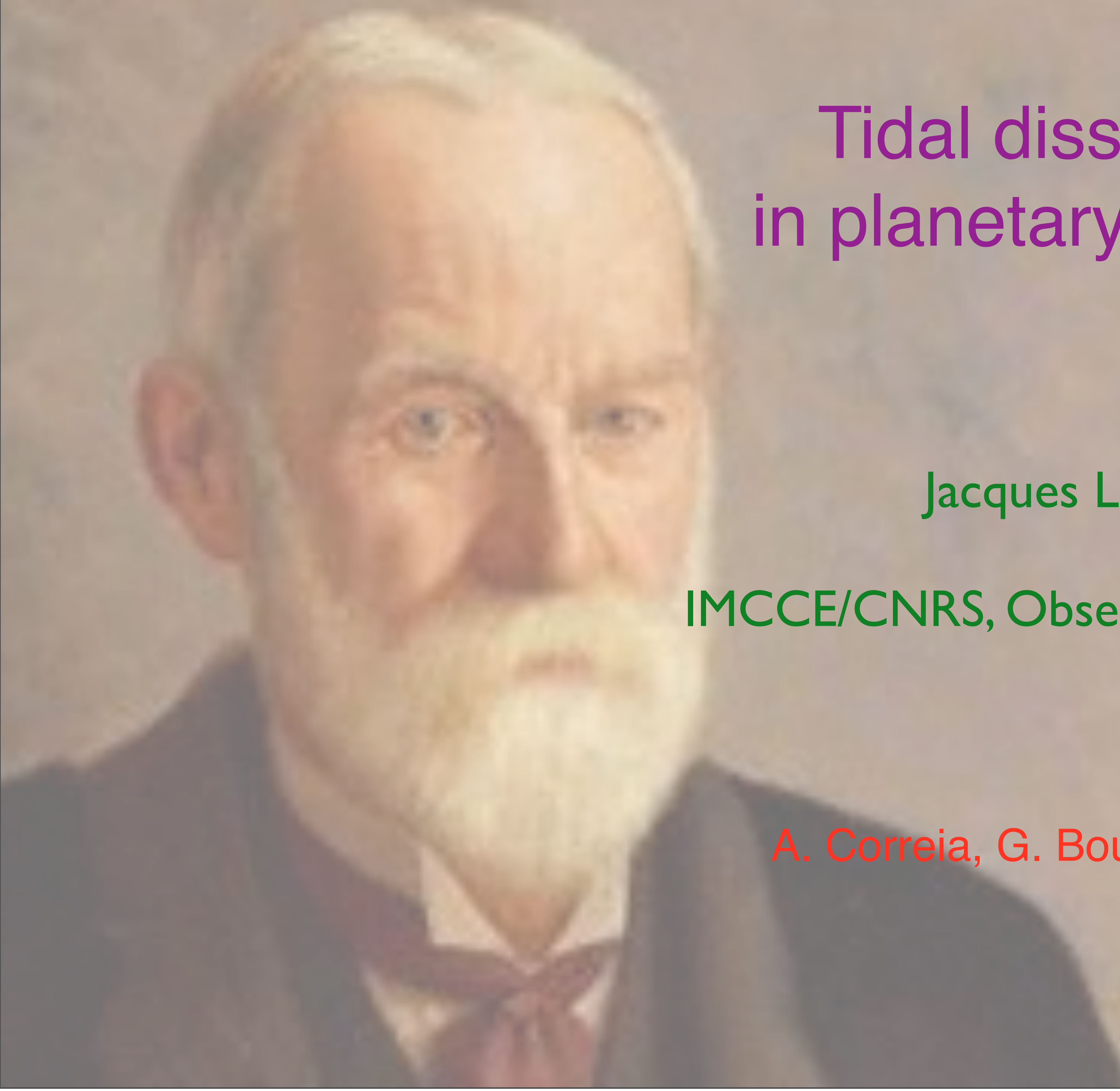

Tidal dissipation in planetary motions

Jacques Laskar

IMCCE/CNRS, Observatoire de Paris

A. Correia, G. Boué, JB Delisle

Tidal dissipation in the Earth-Moon System

BULLETIN OF THE ASTRONOMICAL INSTITUTES OF THE NETHERLANDS.

1927 June 8 Volume IV. No. 124.

COMMUNICATION FROM THE OBSERVATORY AT LEIDEN.

On the secular accelerations and the fluctuations of the longitudes of the moon, the sun, Mercury and Venus, by *W. de Sitter*.

THE ROTATION OF THE EARTH, AND THE SECULAR ACCELERATIONS OF THE SUN, MOON AND PLANETS

H. Spencer Jones, F.R.S., Astronomer Royal (1939)

1. It has been fully established by the researches of various investigators that there are fluctuations in the longitudes of the Sun, Mercury and Venus, which run closely parallel to the fluctuations in the longitude of the Moon. The fluctuations in the longitudes of these several bodies have therefore been attributed to a common cause, a variation of the adopted unit of time provided by the rotation of the Earth.

Zeitschrift für Astrophysik, Bd. 36. S. 245—274 (1955).

About tidal friction in the two-body problem

Über Gezeitenreibung beim Zweikörperproblem.

Von

Horst Gerstenkorn, Hannover.

Mit 4 Textabbildungen.

(Eingegangen am 13. Dezember 1954.)

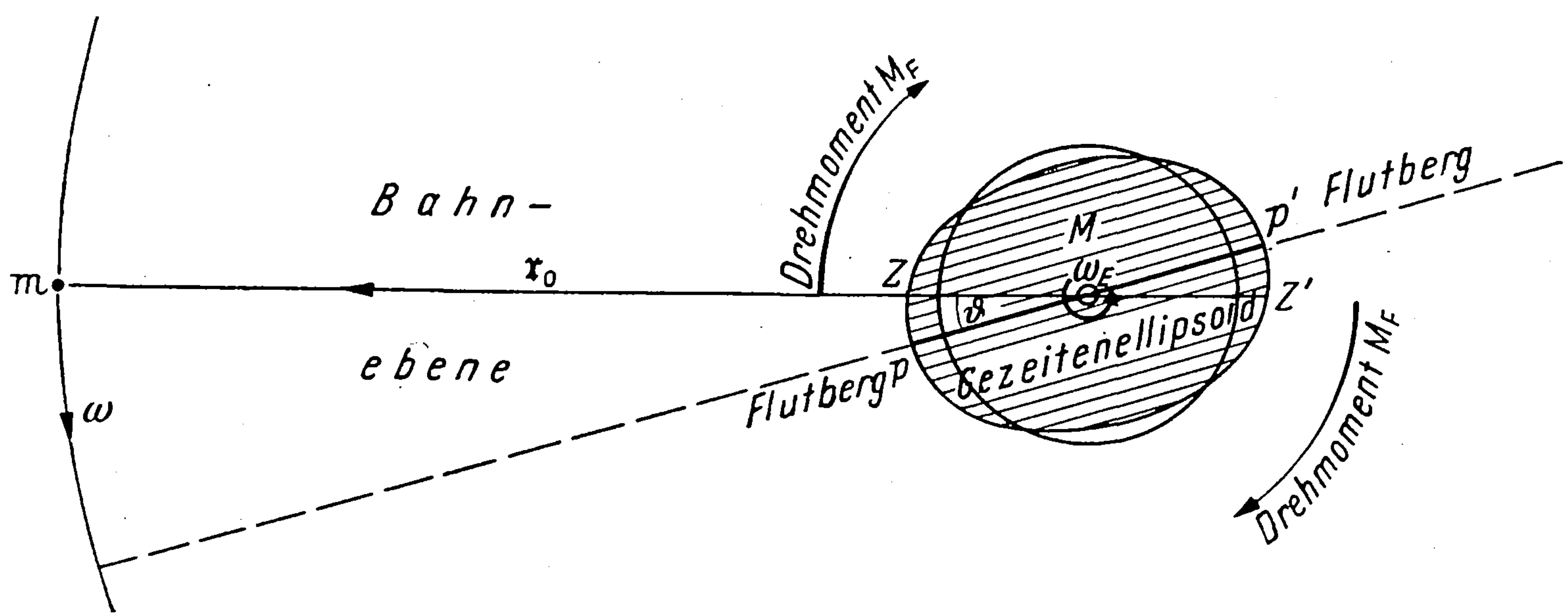

Abb. 1. Das Zustandekommen des Bremsmomentes.

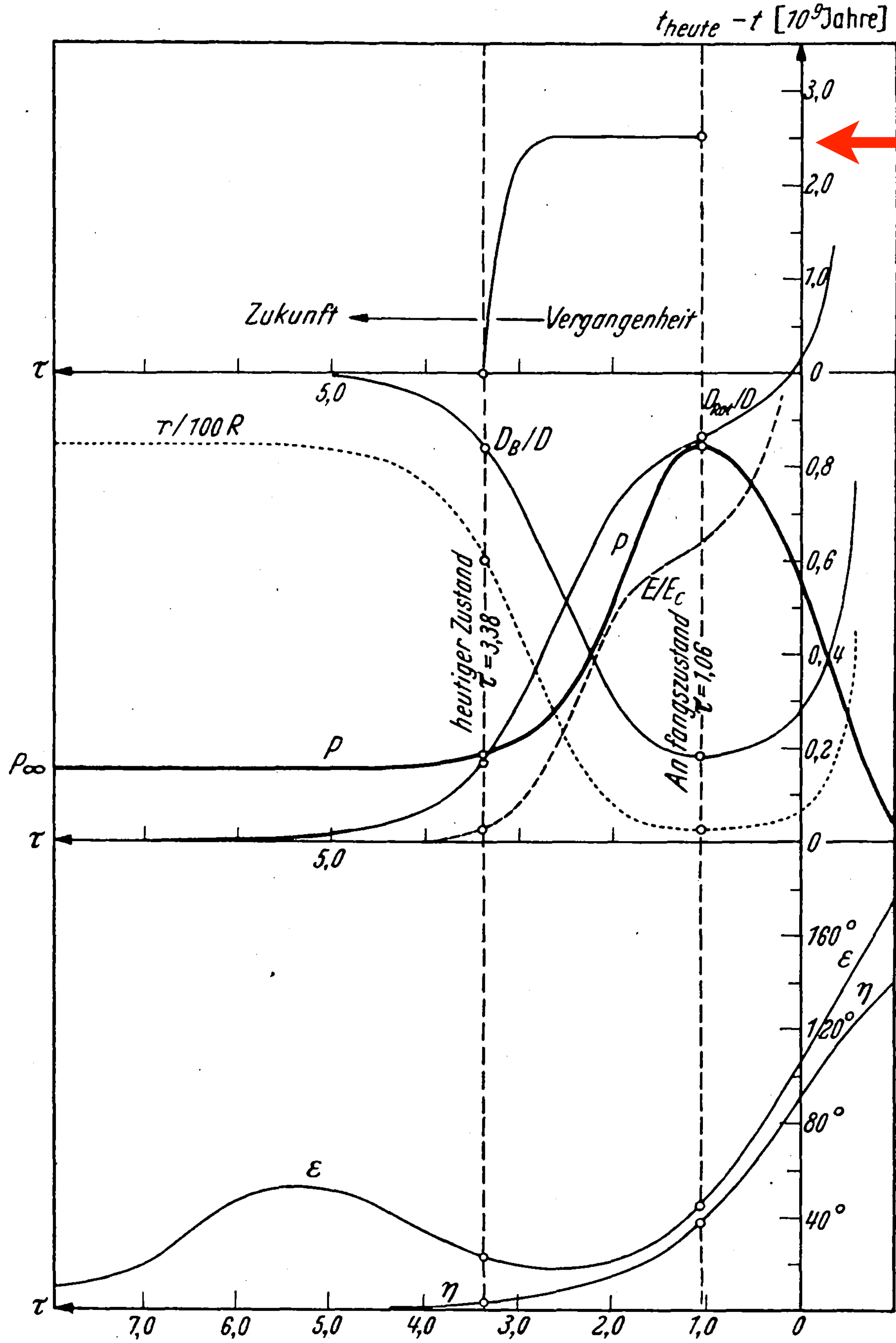

2.5 Gyr

(Gersternkorn, 1955)

Abb. 3. Die Elemente des Systems Erde—Mond. Als Abszisse wurde der Parameter τ aufgetragen. $\tau = 3.38$ entspricht dem heutigen Zustand. Der Mittelteil der Abbildung enthält als Ordinate zunächst die Lösung $p(\tau)$, die gemäß (13) die dritte Wurzel der Umlaufsfrequenz in der speziellen Einheit darstellt. Aus dieser Kurve sind die anderen abgeleitet. Den Zusammenhang zwischen τ und der Zeit t veranschaulicht der obere Teil der Abbildung; Beachtung verdient die relative Kürze des zwischen $\tau = 1.06$ und $\tau = 2.60$ verstrichenen Zeitraumes. Der untere Teil der Abbildung zeigt die Winkel $\varepsilon = \mathfrak{D}_B, \mathfrak{D}_{Rot}$ und $\eta = \sphericalangle\, \mathfrak{D}_B, \mathfrak{D}$. Im Mittelteil sind ferner dargestellt das Verhältnis a/R Bahn- zu Erdradius, das bei $\tau = 1.06$ den Minimalwert 2.89 besitzt, ferner die mechanische Energie des Systems und die Drehimpulse D_B und D_{Rot} der Bahn und der Eigenrotation, beide auf den Gesamtdrehimpuls D bezogen.

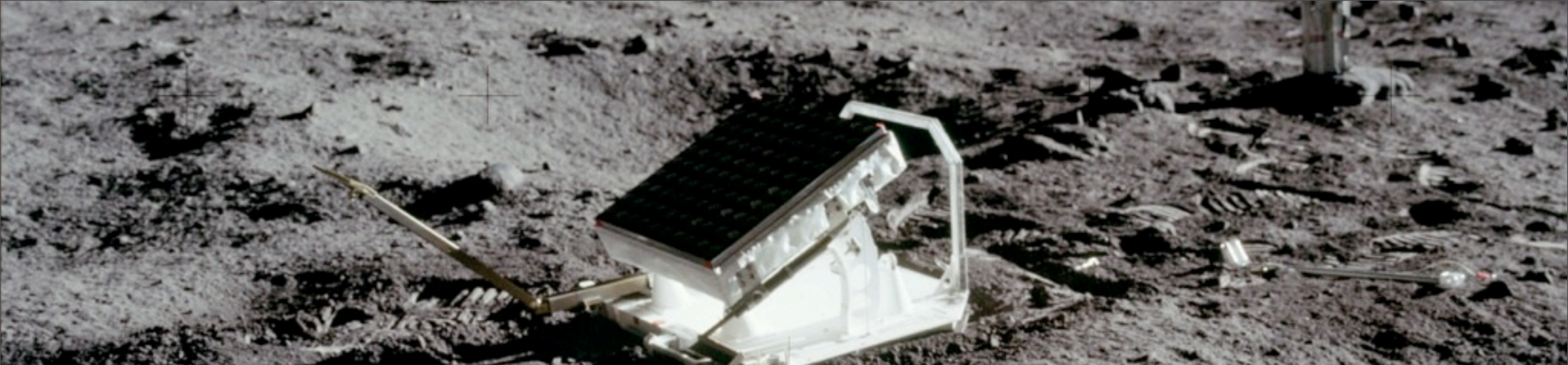

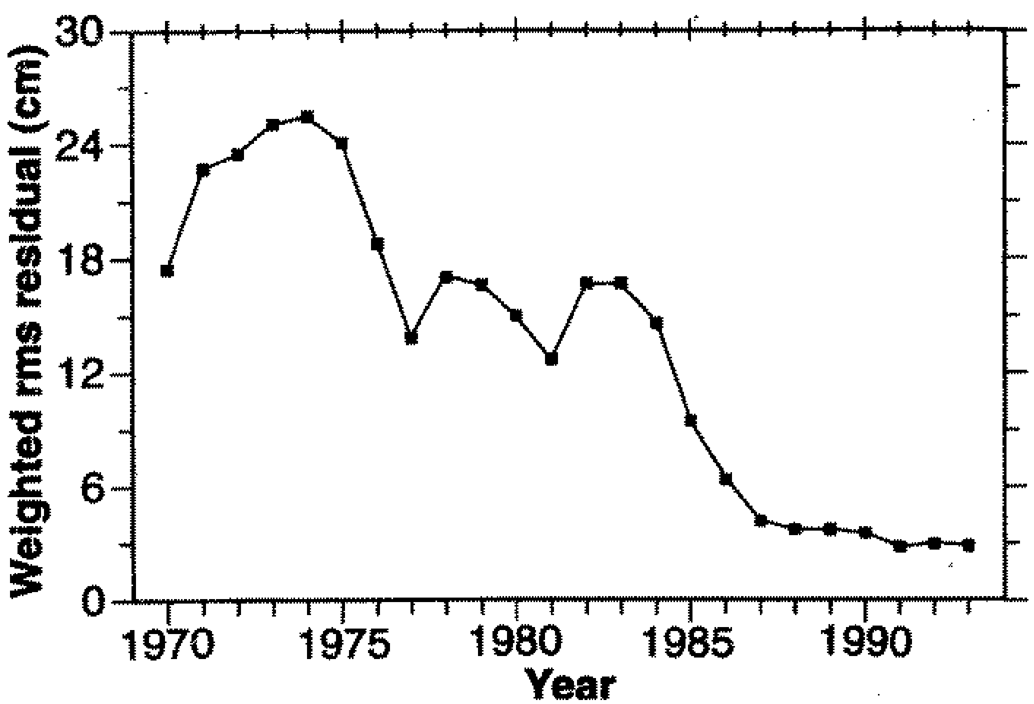

Fig. 2. Histogram of the weighted root-mean-square (rms) post-fit residual (observed minus model) as a function of time.

Dickey et al, 1994

Cerga

INPOP07 LLR residuals Grasse

(H. Manche, IMCCE, S. Bouquillon, SYRTE)

8262 pts moy: 0.011 cm sig: 4.64 cm (4.4 cm)

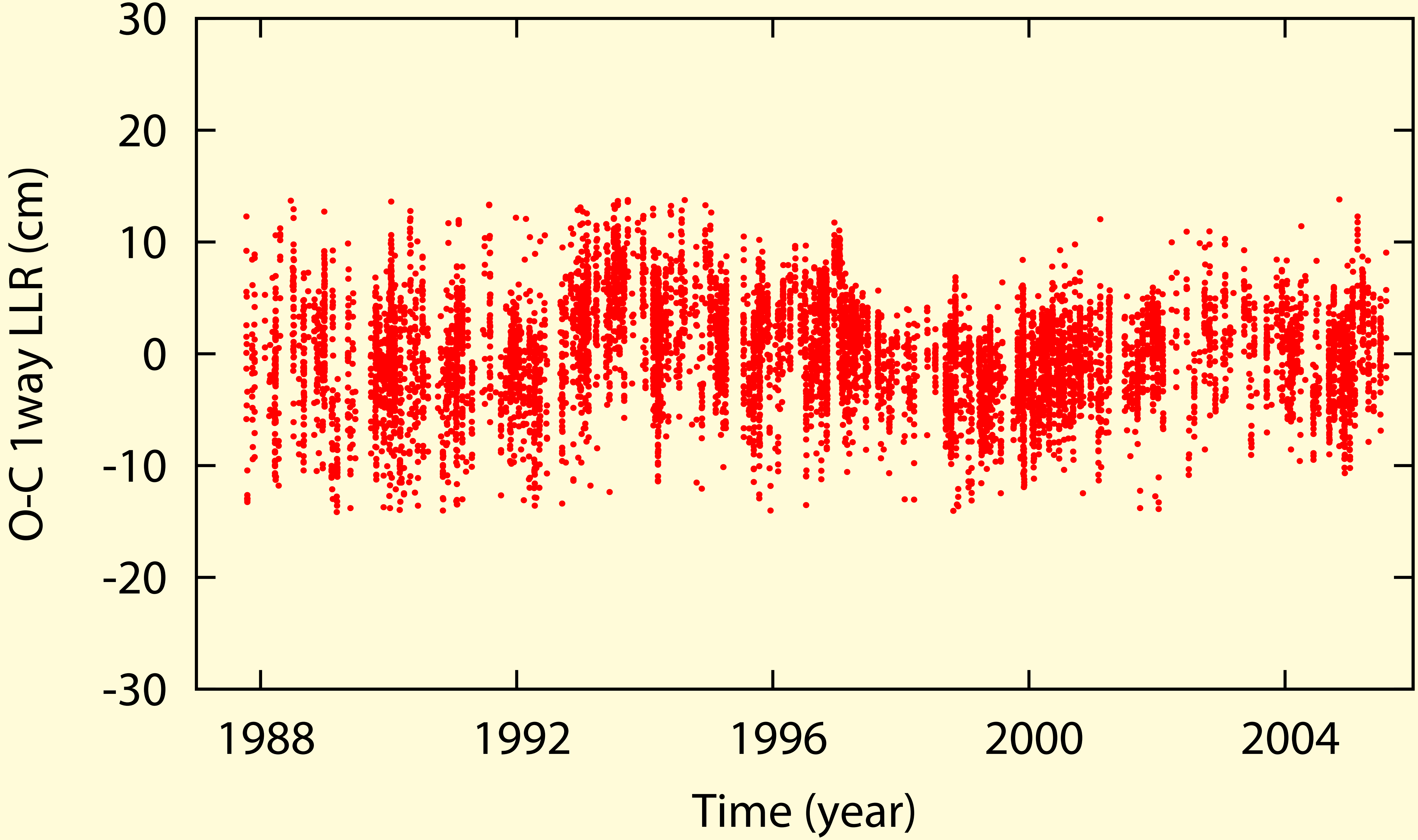

Geophys. J. R. astr. Soc. (1982) 70, 261–271

Tides and the evolution of the Earth–Moon system

D. J. Webb *Institute of Oceanographic Sciences, Wormley, Godalming GU8 5UB*

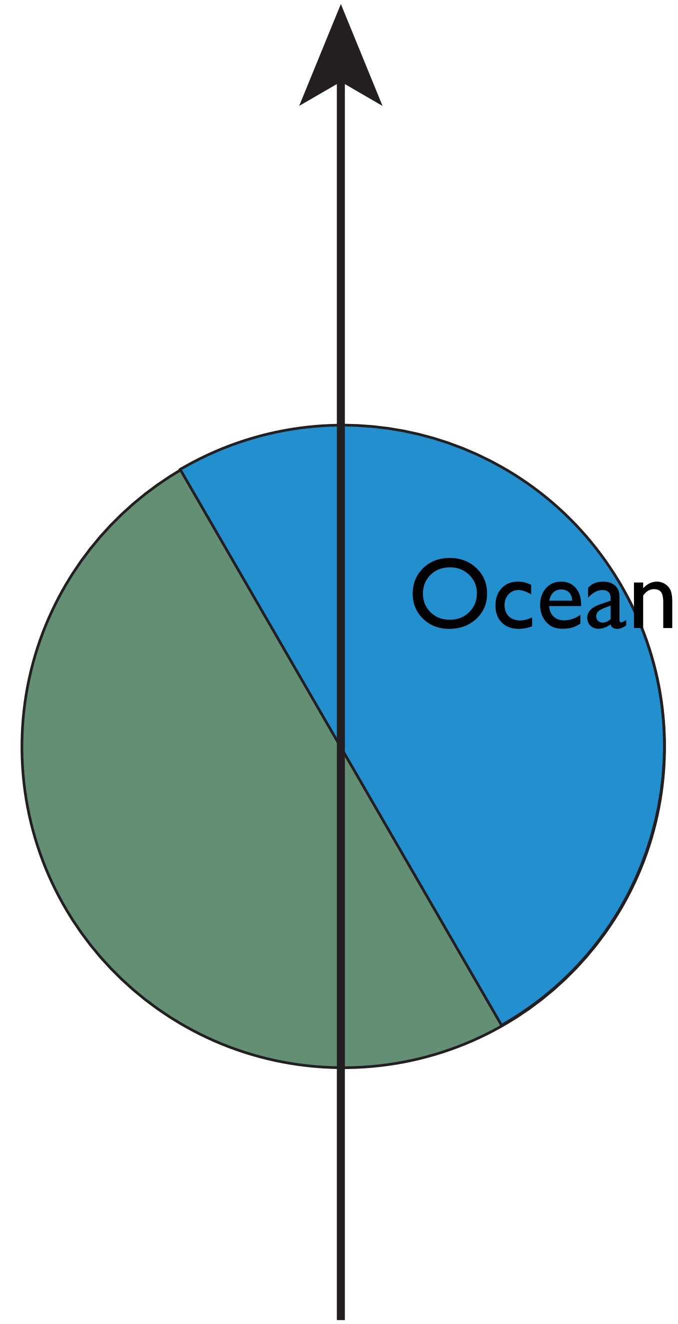

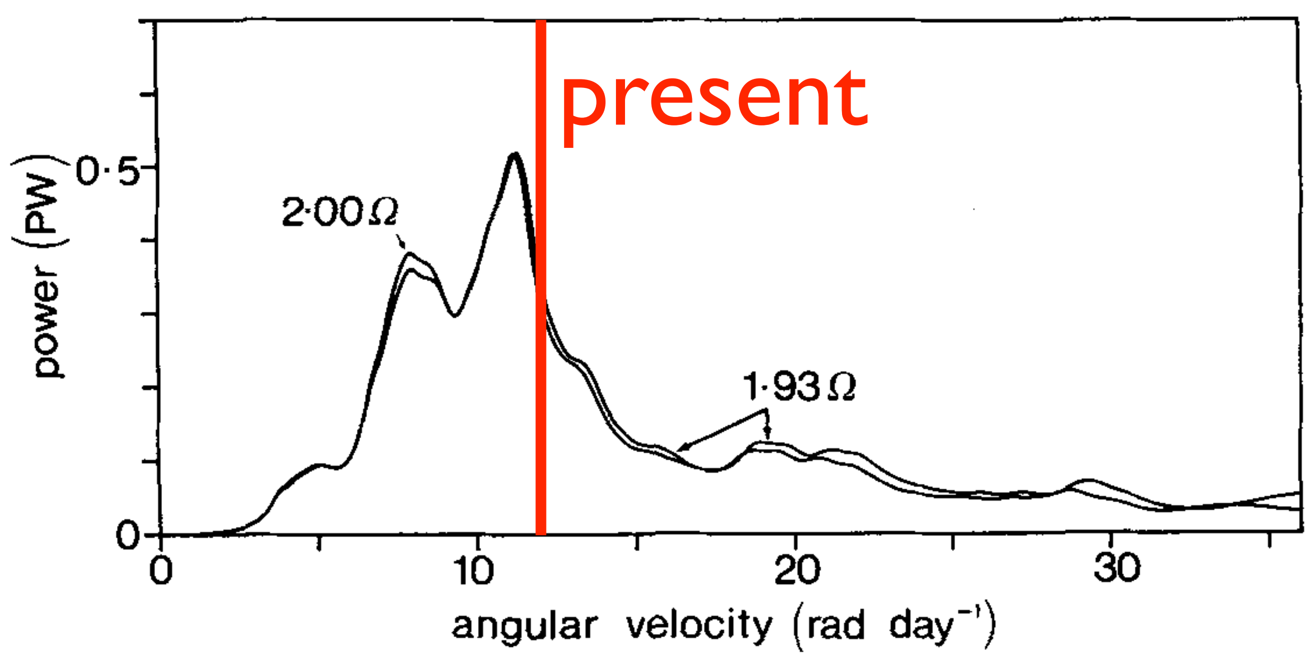

Figure 2. The average power dissipation curves plotted as a function of the angular velocity of the tide for the two cases when ω is equal to $1.93\,\Omega$ and $1.00\,\Omega$. The power is in petawatts and the angular velocity is in units of radians per present Earth day.

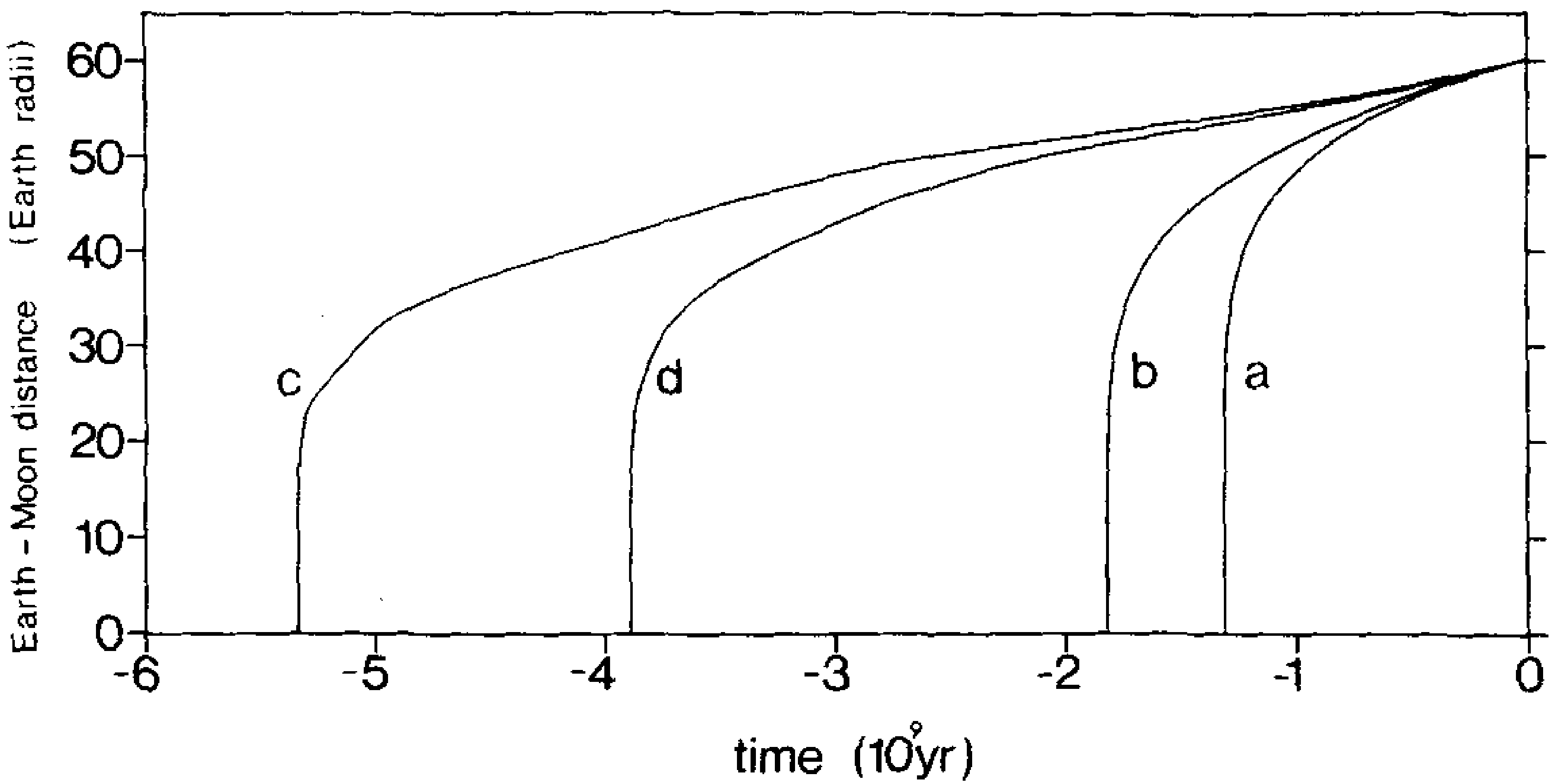

Figure 3. The Earth–Moon separation measured in Earth radii and plotted as a function of time for the cases: (a) torque independent of frequency, (b) power dissipated independent of frequency, (c) power dissipation from ocean model, (d) power dissipation in both the ocean and the solid Earth.

geological observations

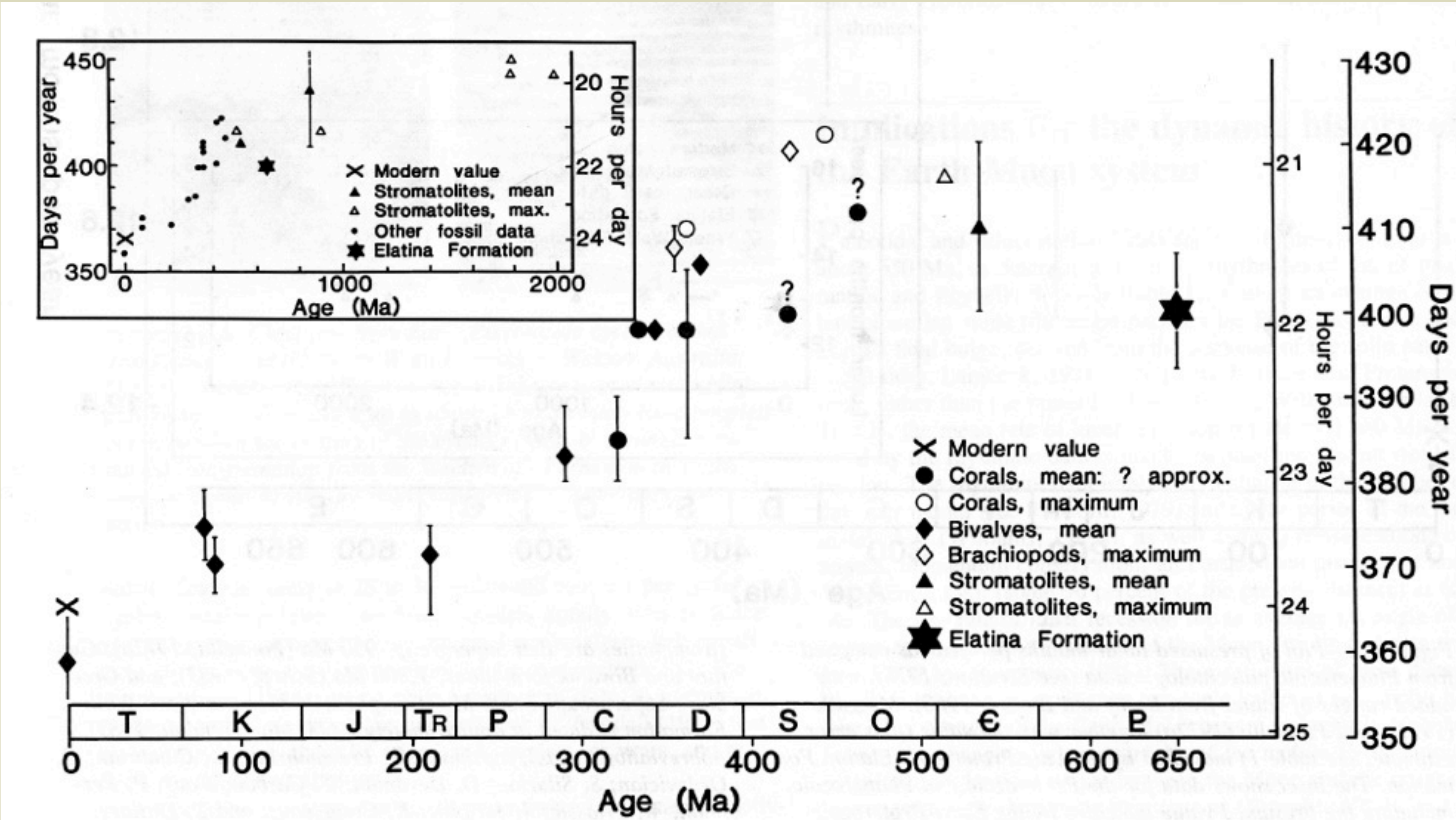

G. Williams, *Episodes*, 1989

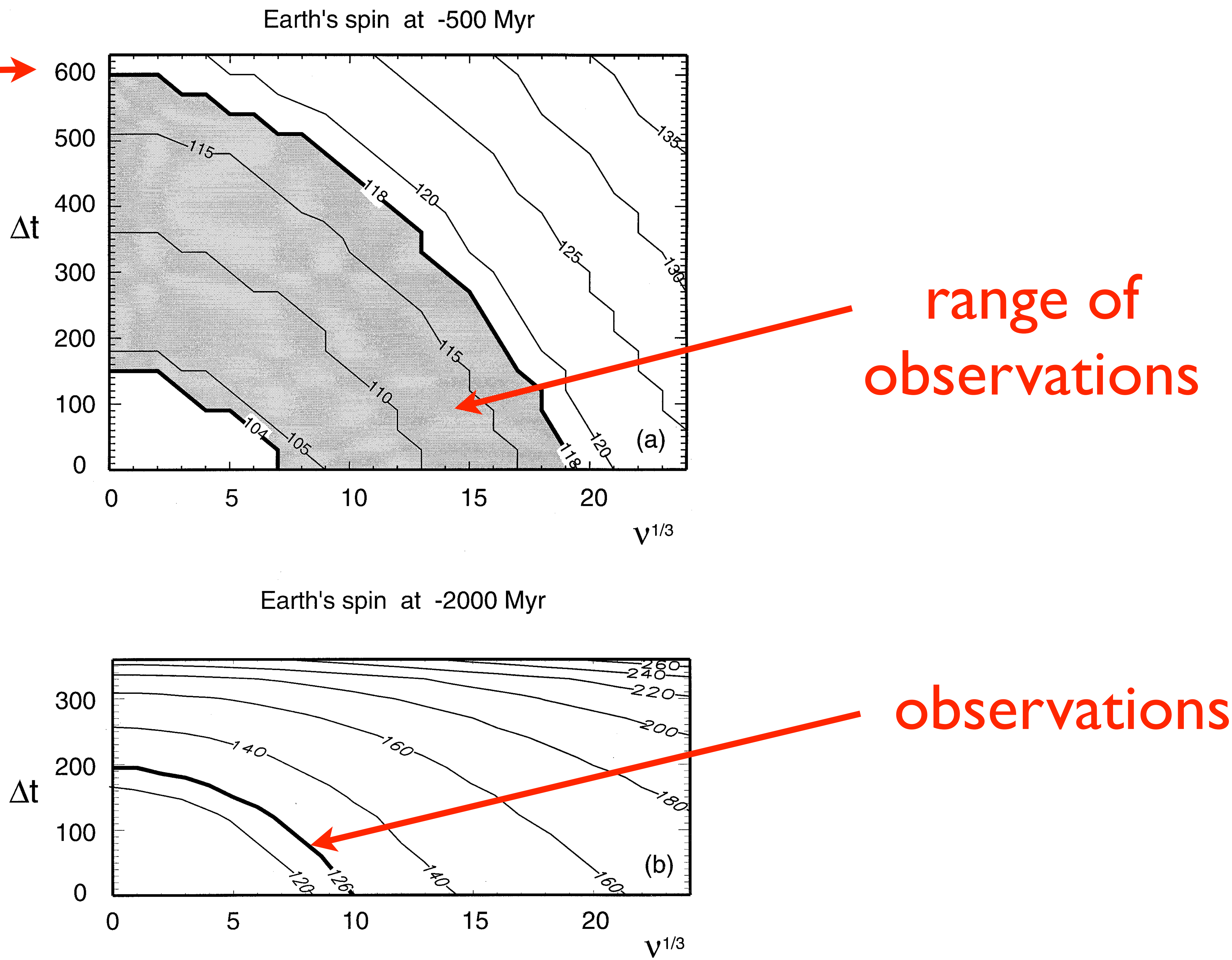

Fig. 3. a Percentage of the ratio of the speed of rotation at −500 Myr over the present one for various values of the tidal delay Δt and the viscosity ν. The two bold lines delimit an acceptable range, in agreement with the observations from sediments and fossils. **b** Same percentage at −2 000 Myr. The bold line corresponds to the observation of Williams (1989).

Néron de Surgy & Laskar, 1997

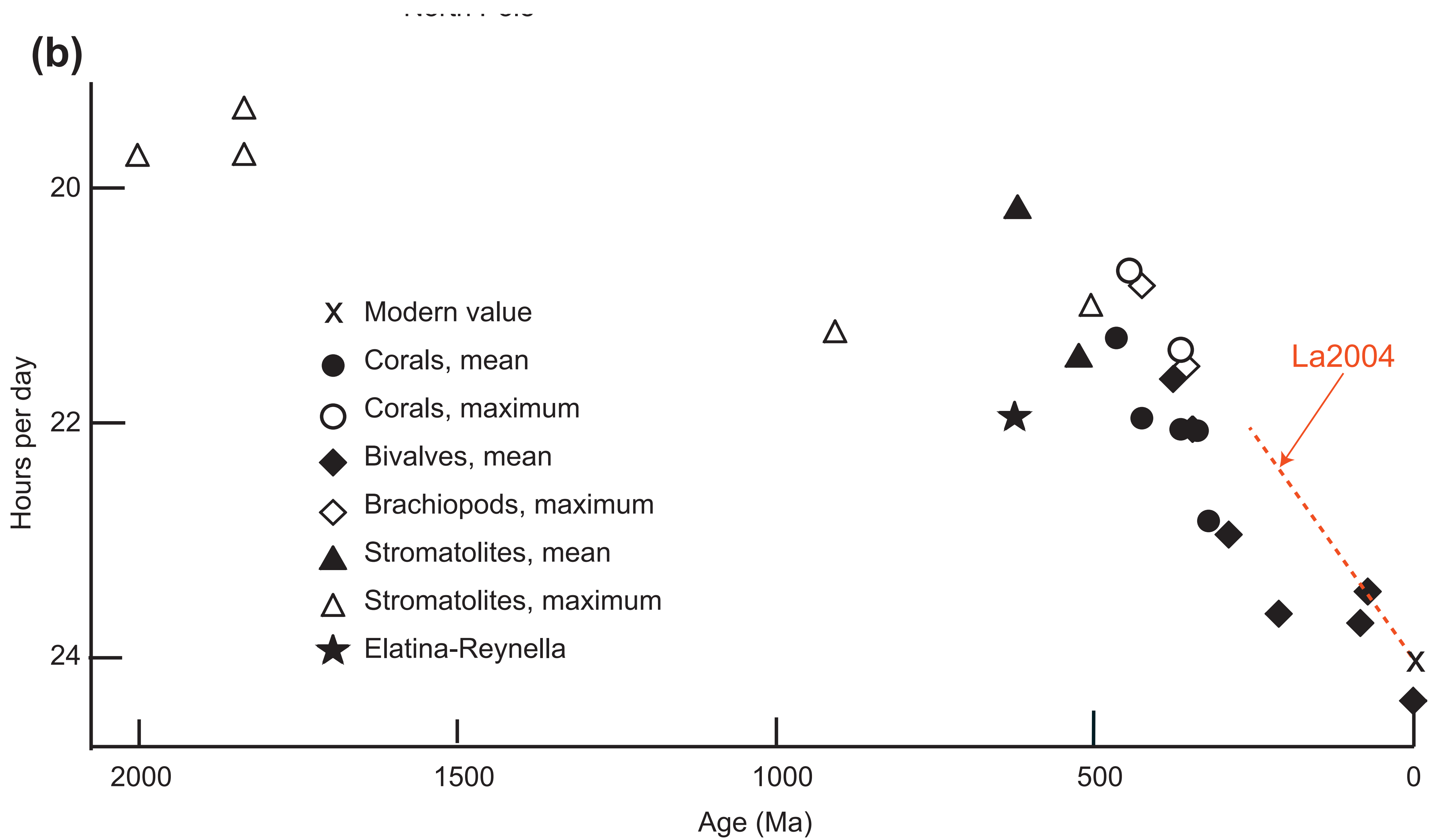

FIGURE 4.9 **Earth rotation deceleration from tidal energy dissipation.** *(a)* The Moon raises a tidal bulge that is delayed due to friction between the oceans and crust, and within the solid Earth, by an angle δ, which is 0.2° for the solid M_2 tide and ~65° for the net ocean M_2 tide (Munk, 1997; Ray et al., 2001). Gravitational force from the Moon acts on the offset bulge, producing a torque on the Earth in a direction opposite from the rotation, causing the Earth to decelerate. *(b)* Deceleration of the Earth over the past 2 billion years based on geological data. The data shown are from Williams (2000). Corals, bivalves and brachiopods secrete daily growth bands that modulate annually; fossils indicate more growth bands per year back in time. Stromatolite laminations have been interpreted similarly. Tidalites are an alternate, relatively rare source of information. The red dashed line indicates the length-of-day model used in the nominal La2004 solution of Laskar *et al.* (2004), which assumes present-day tidal dissipation and dynamical ellipticity. Table 4.2 lists obliquity and precession periodicities for key geological times.

Hinnov, in Gradstein et al, 2012

ELSEVIER
2009 Earth-Science Reviews
journal homepage: www.elsevier.com/locate/earscirev

Tides, tidalites, and secular changes in the Earth–Moon system

Christopher L. Coughenour [a], Allen W. Archer [b], Kenneth J. Lacovara [c,*]

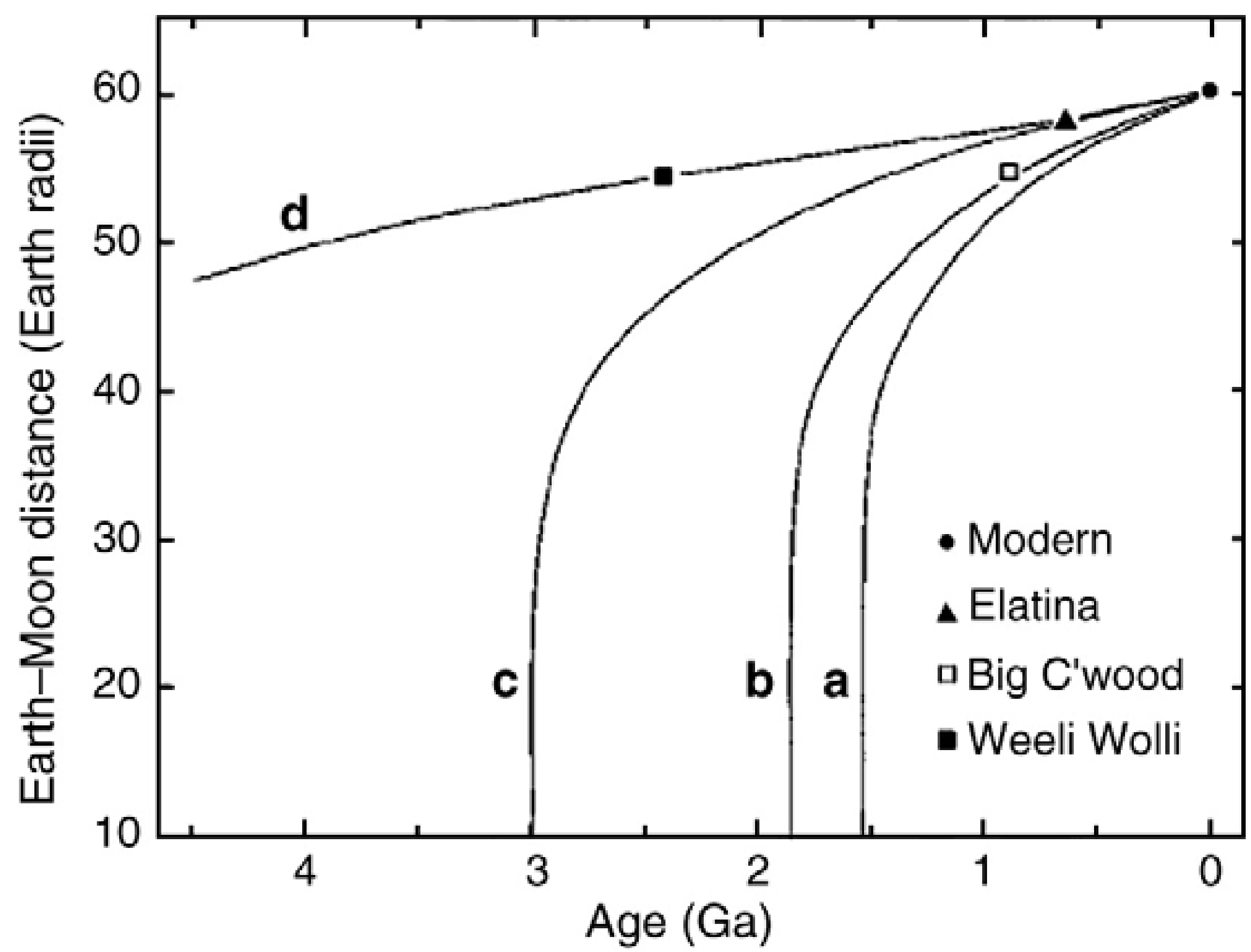

Fig. 11. Several possible scenarios of lunar recession as interpolated from Precambrian tidal rhythmite data. Curve a is the predicted history of recession assuming the present rate of dissipation. Curve b is the predicted recession the mean rate of dissipation from

Tidal dissipation

Darwin, 1880; Gersternkorn, 1955; Kaula, 1964; Goldreich, 1966; Mignard, 1979,80,81; Hut, 1981; Touma & Wisdom, 1994; Néron de Surgy & Laskar, 1997; Efroimsky & Williams, 2009; Ferraz-Mello, 2013; Correia, Boué, Laskar, Rodriguez, 2014;

Text

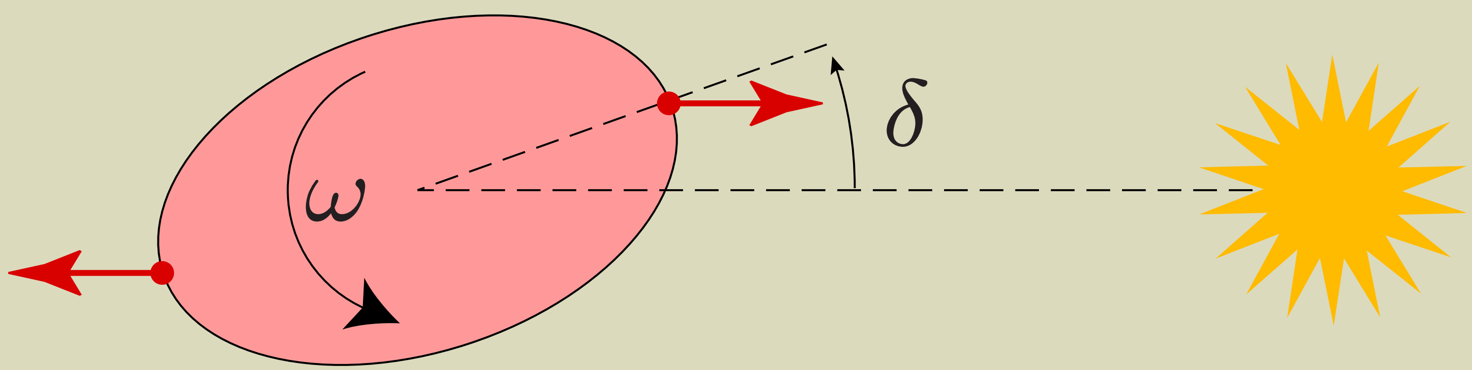

Precession (ψ) and obliquity ($X = \cos\varepsilon$)

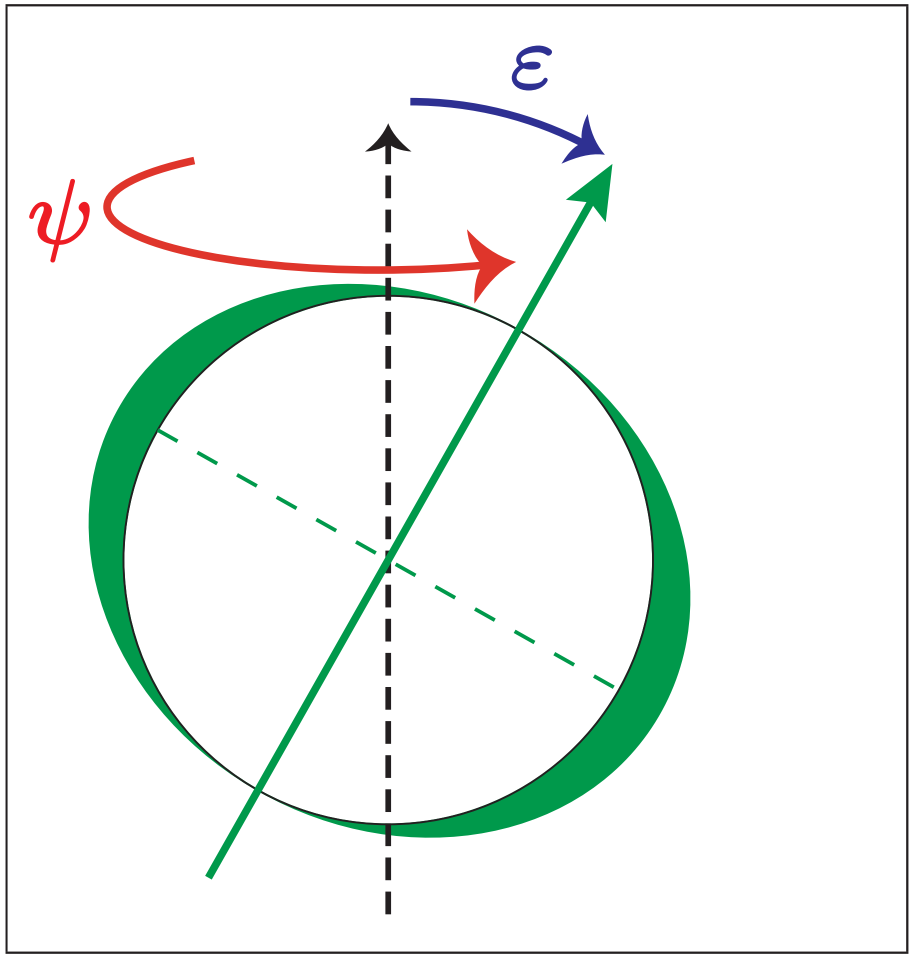

$$\dot\psi = \alpha \cos \varepsilon_0$$

$$H = \frac{1}{2}\alpha\, X^2$$

$$\begin{cases} \dfrac{d\psi}{dt} = \dfrac{\partial H}{\partial X} = \alpha\, X_0 \\[2ex] \dfrac{dX}{dt} = -\dfrac{\partial H}{\partial \psi} = 0 \end{cases}$$

$$\alpha = \frac{3}{2}\frac{k^2}{\nu}\frac{C-A}{C}\left[\frac{m_M}{a_M^3} + \frac{m_\odot}{a_\odot^3}\right]$$

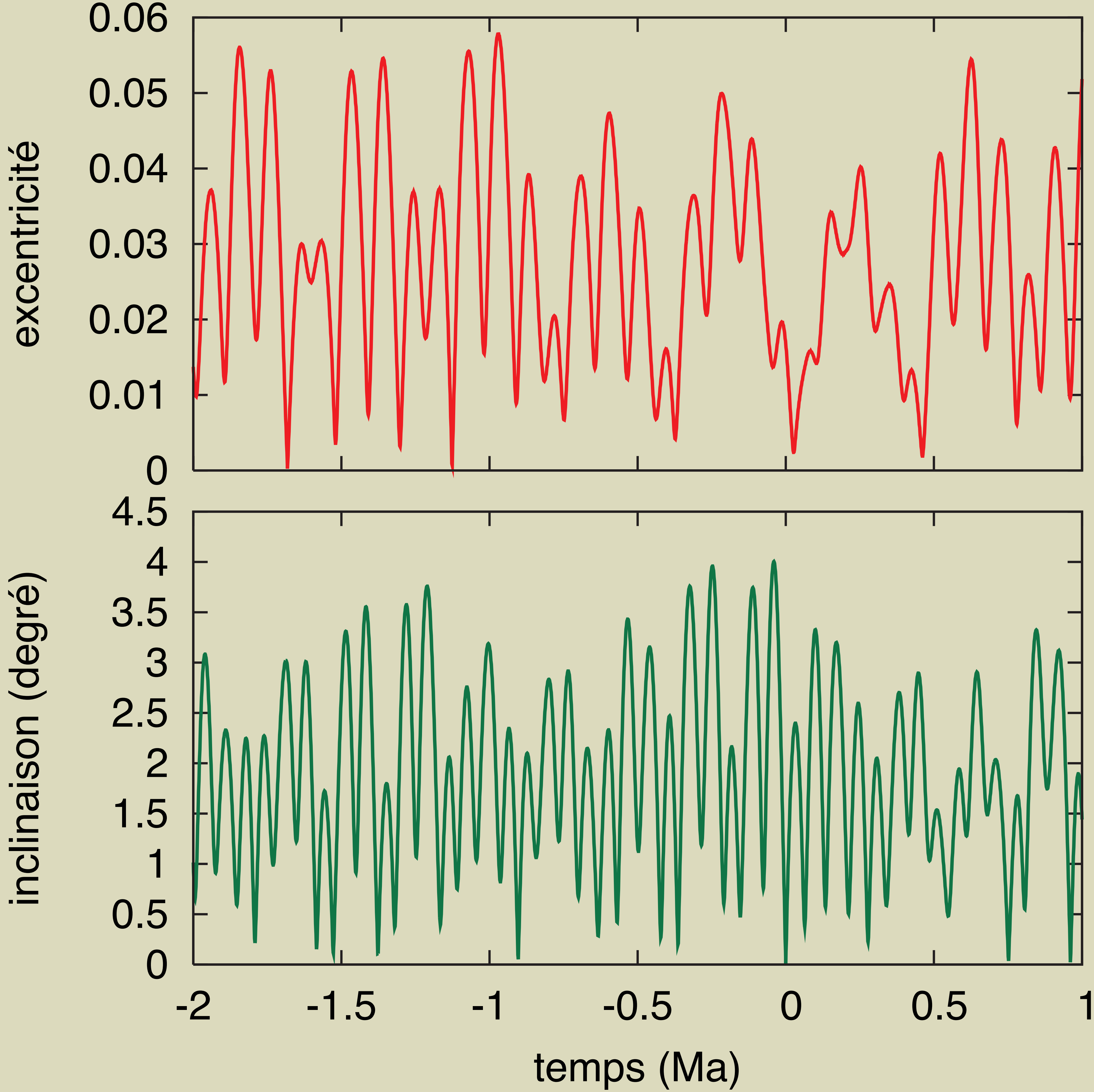
excentricité
0.06
0.05
0.04
0.03
0.02
0.01
0
inclinaison (degré)
4.5
4
3.5
3
2.5
2
1.5
1
0.5
0
-2
-1.5
-1
-0.5
0
0.5
1
temps (Ma)

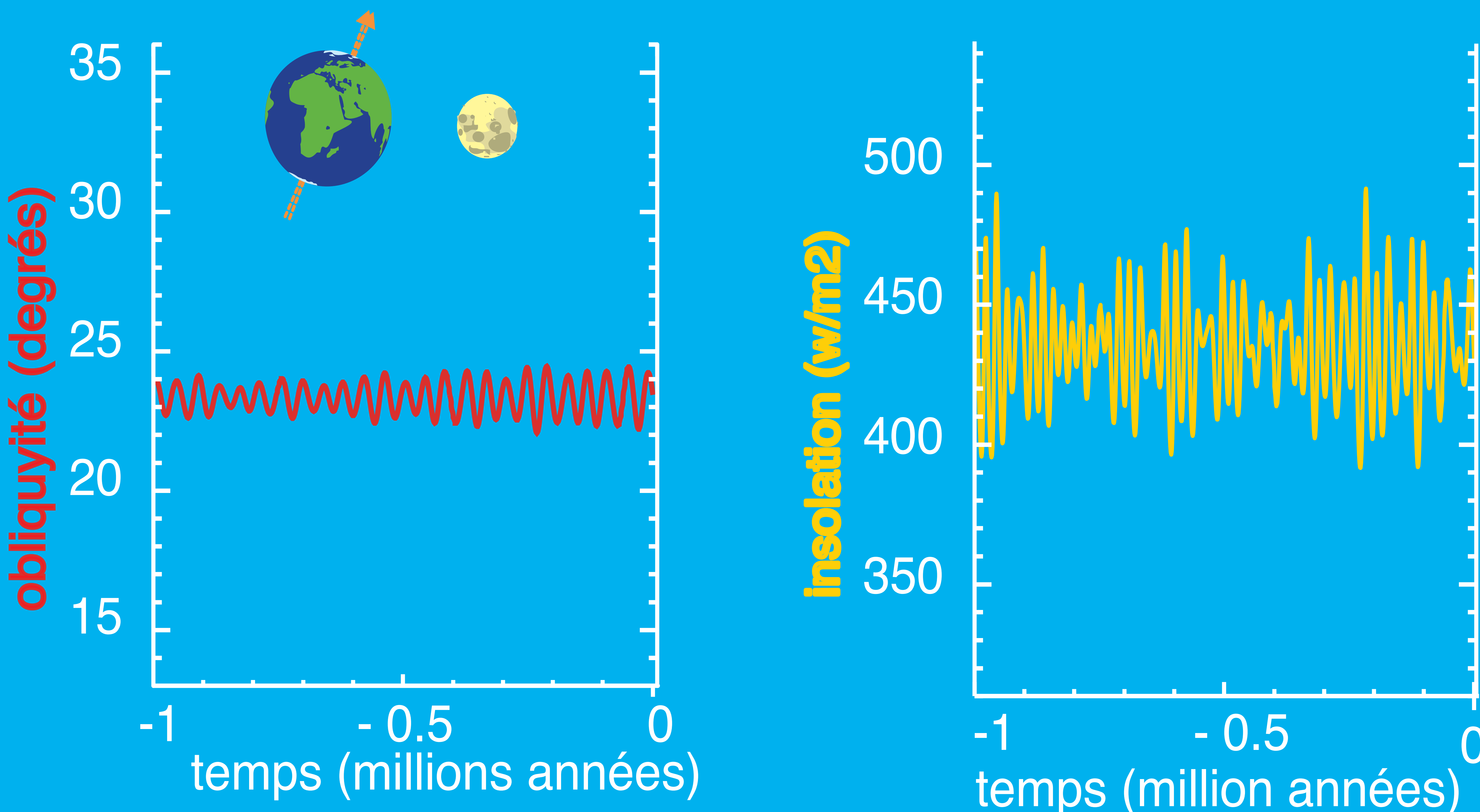

35
30
25
20
15
obliquyité (degrés)
-1
- 0.5
0
temps (millions années)
500
450
400
350
insolation (w/m2)
-1
- 0.5
0
temps (million années)

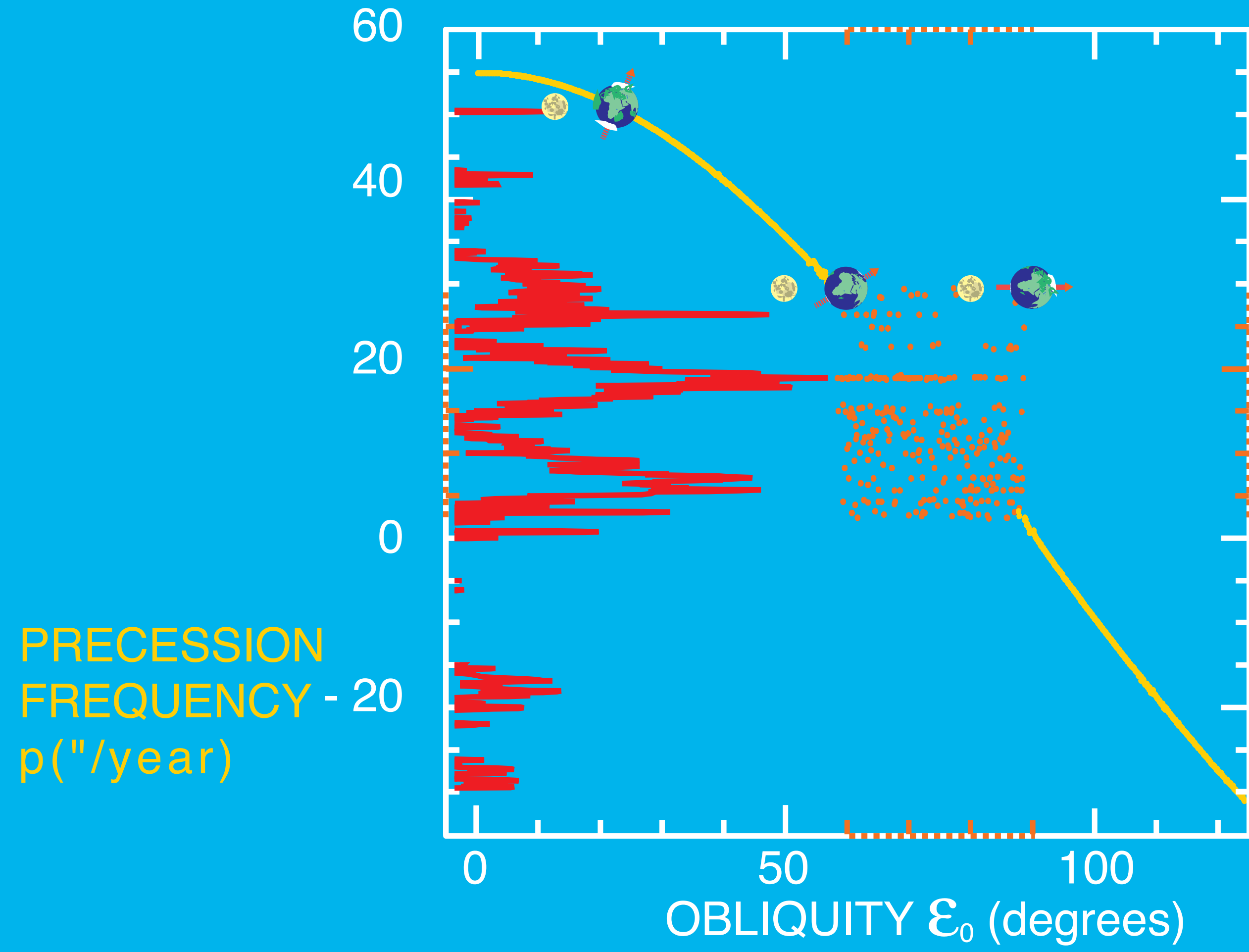

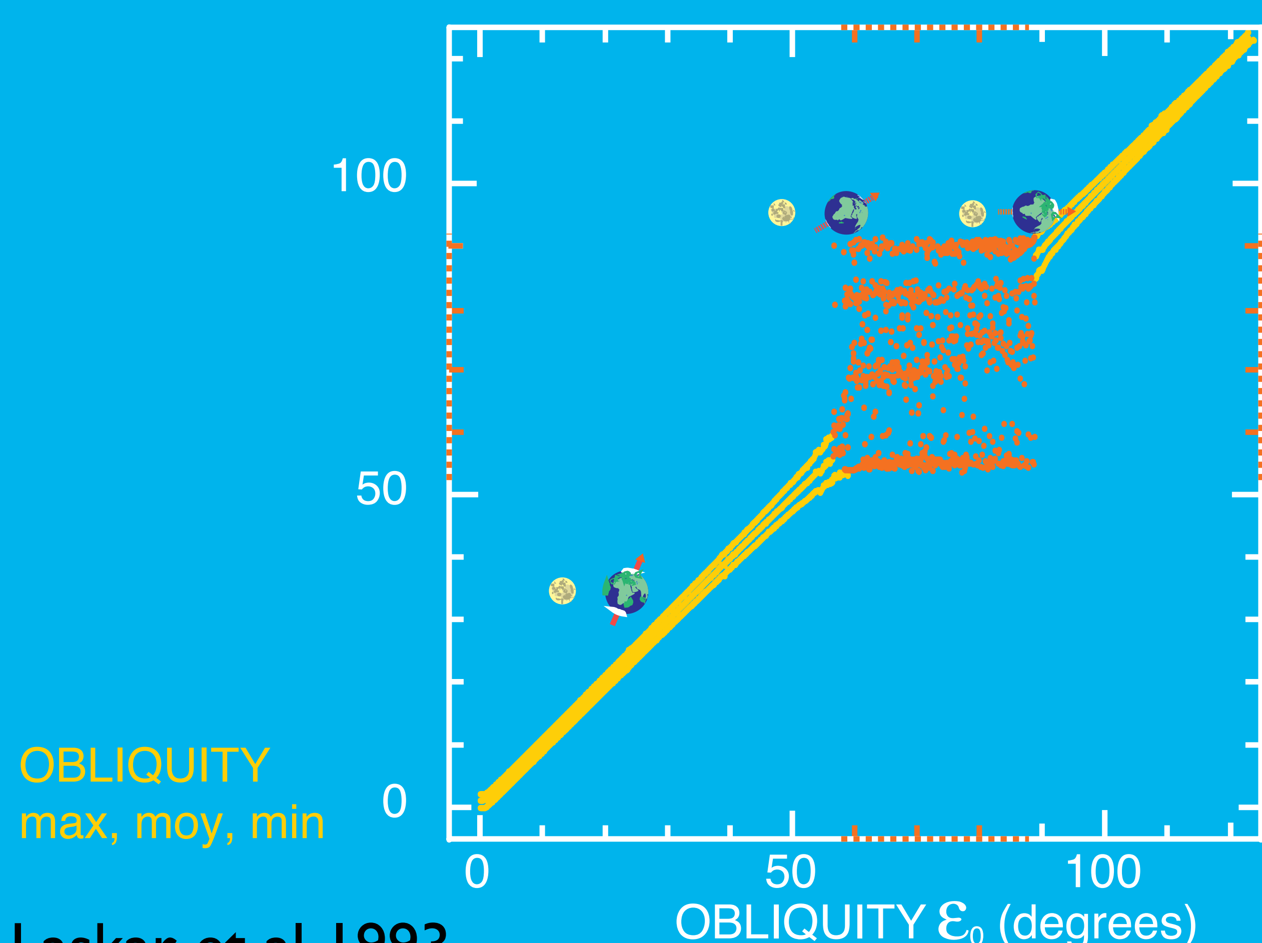

Laskar et al 1993

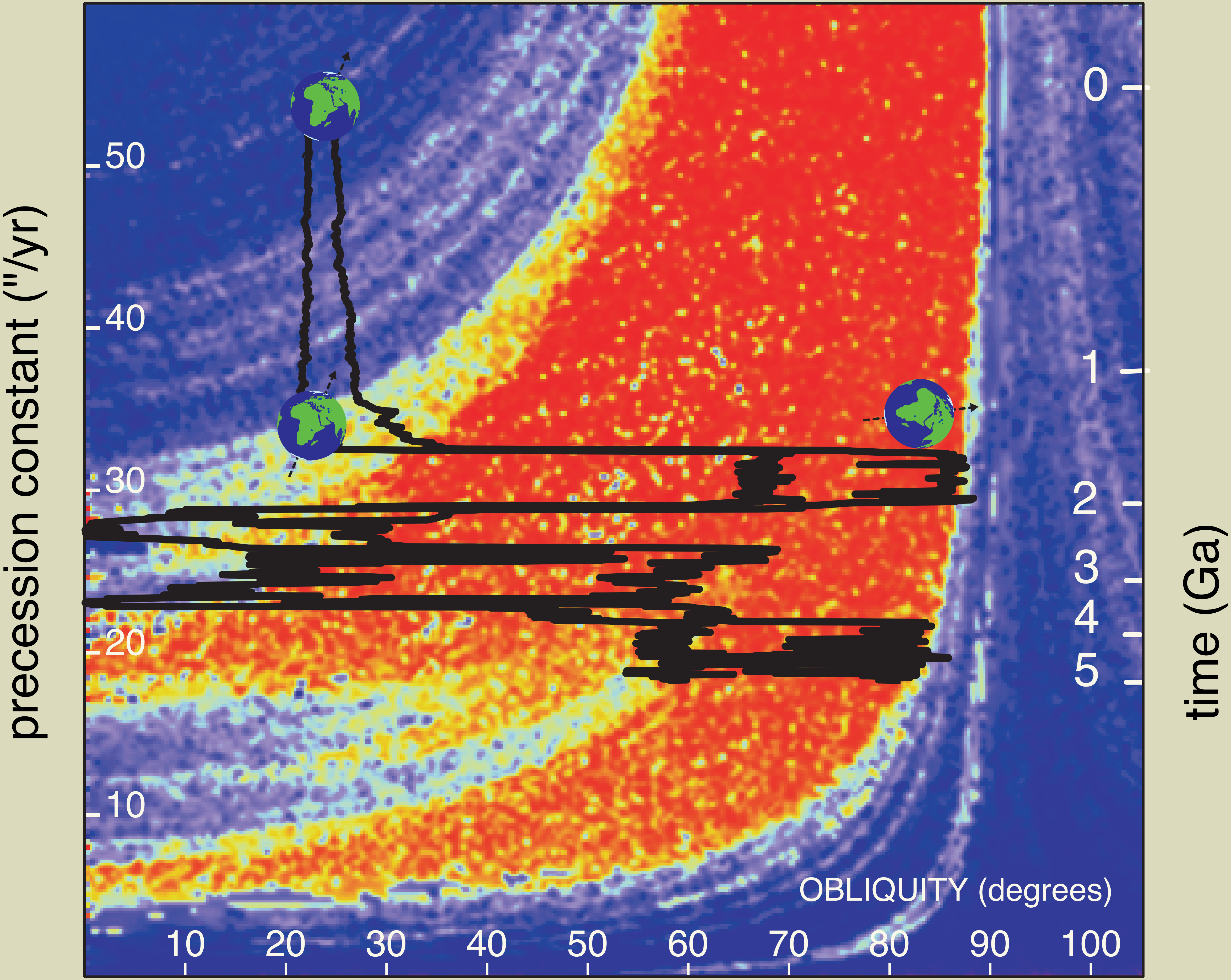

Laskar & Robutel, 1993, Laskar, 1993, Néron de Surgy and Laskar, 1997

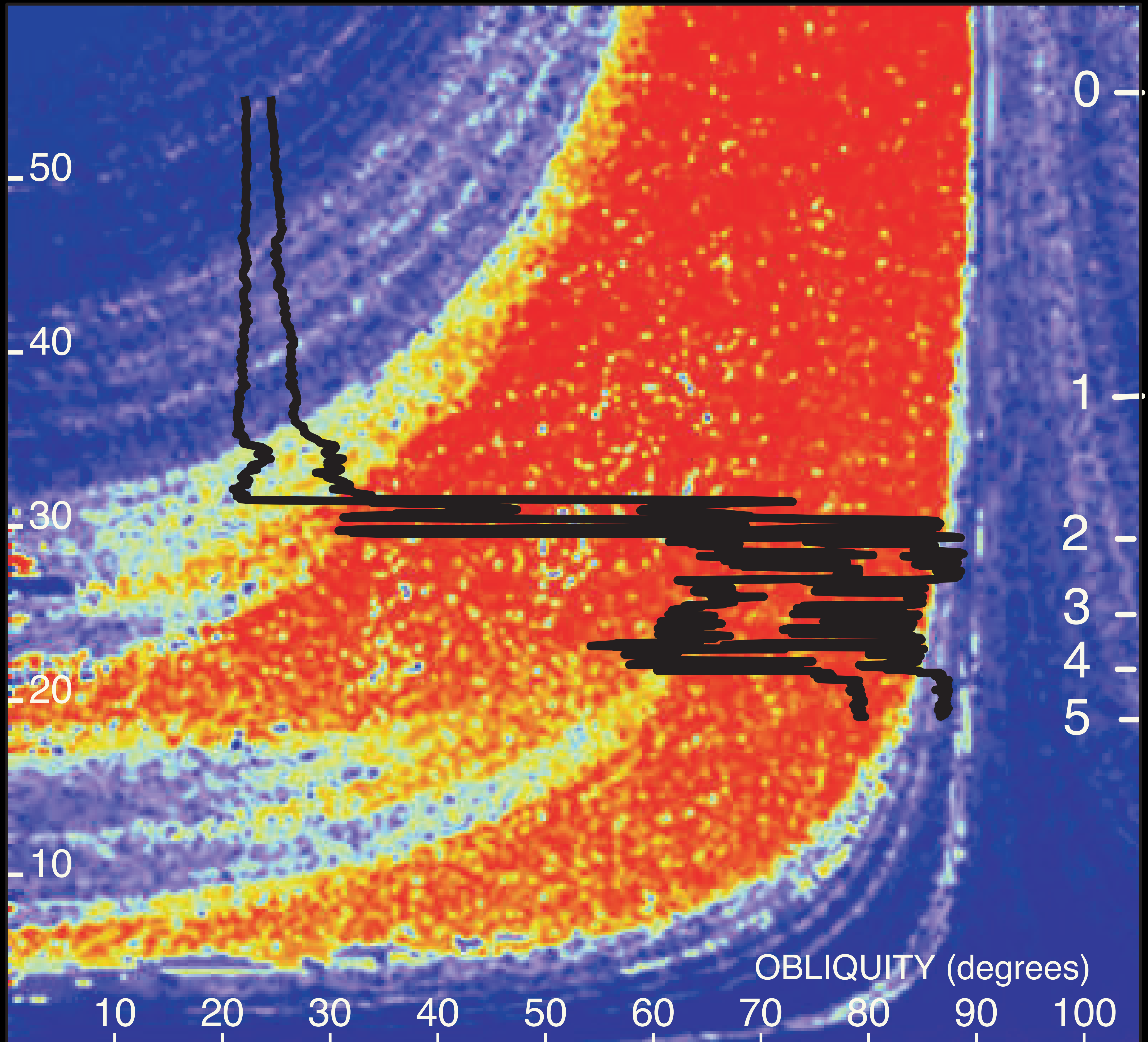

0
1
2
3
4
5
50
40
30
20
10
OBLIQUITY (degrees)
10
20
30
40
50
60
70
80
90
100

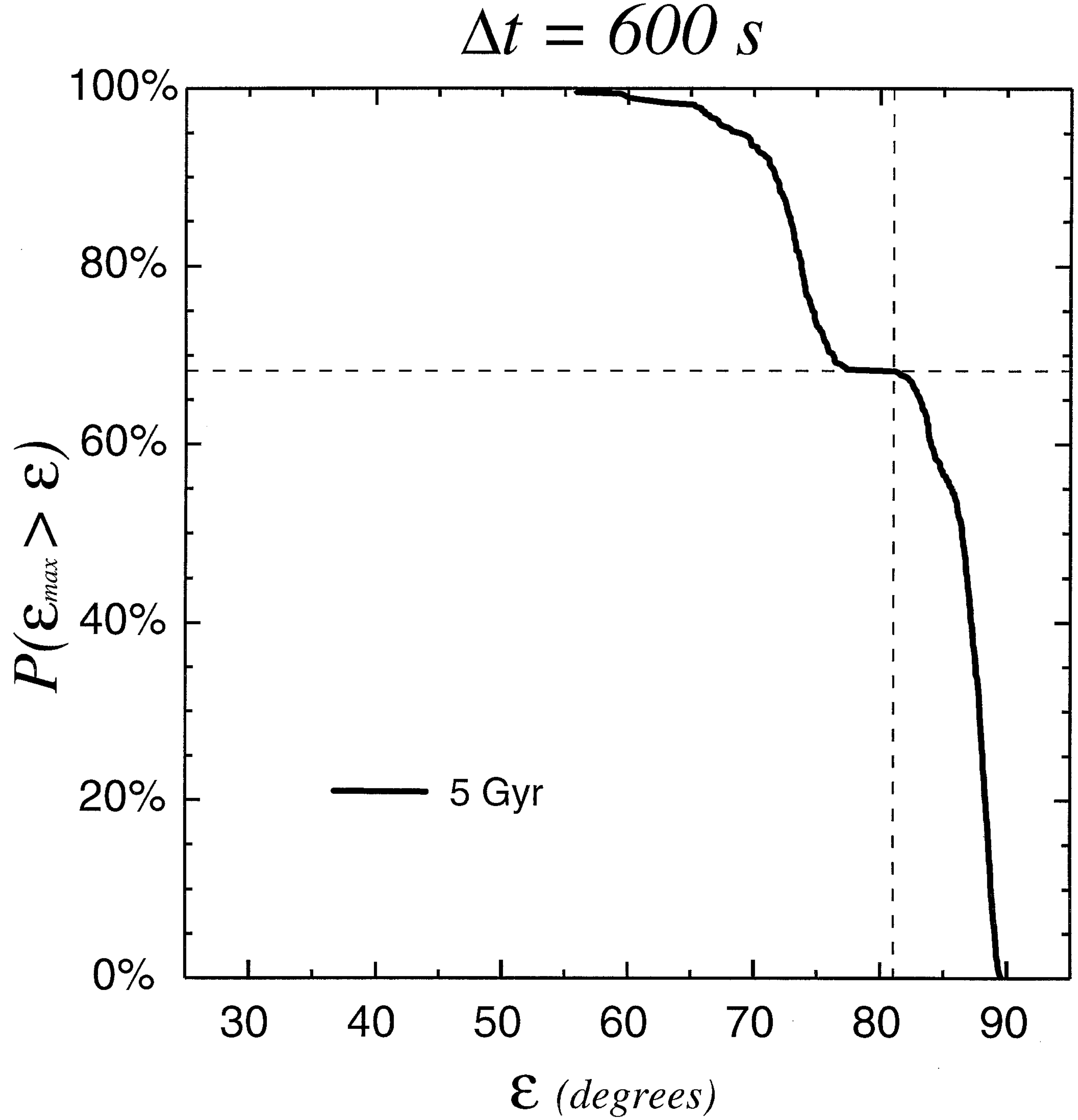

Fig. 5. Probability P for the maximum obliquity ϵ_{max} to exceed a given value ϵ for the Earth with $\Delta t = 600s$. This was performed over 500 orbits with very close initial conditions followed over 5 Gyr.

(Néron de Surgy & Laskar, A&A, 1997)

Terrestrial planets

	Mercury	Venus	Earth	Mars
Obliquity (deg)	0.1	177.3	23.4	25.2
Rot. Period (days)	58.6	243	1.00	1.03
Orb. Period (days)	88.0	224.7	365.2	686.9

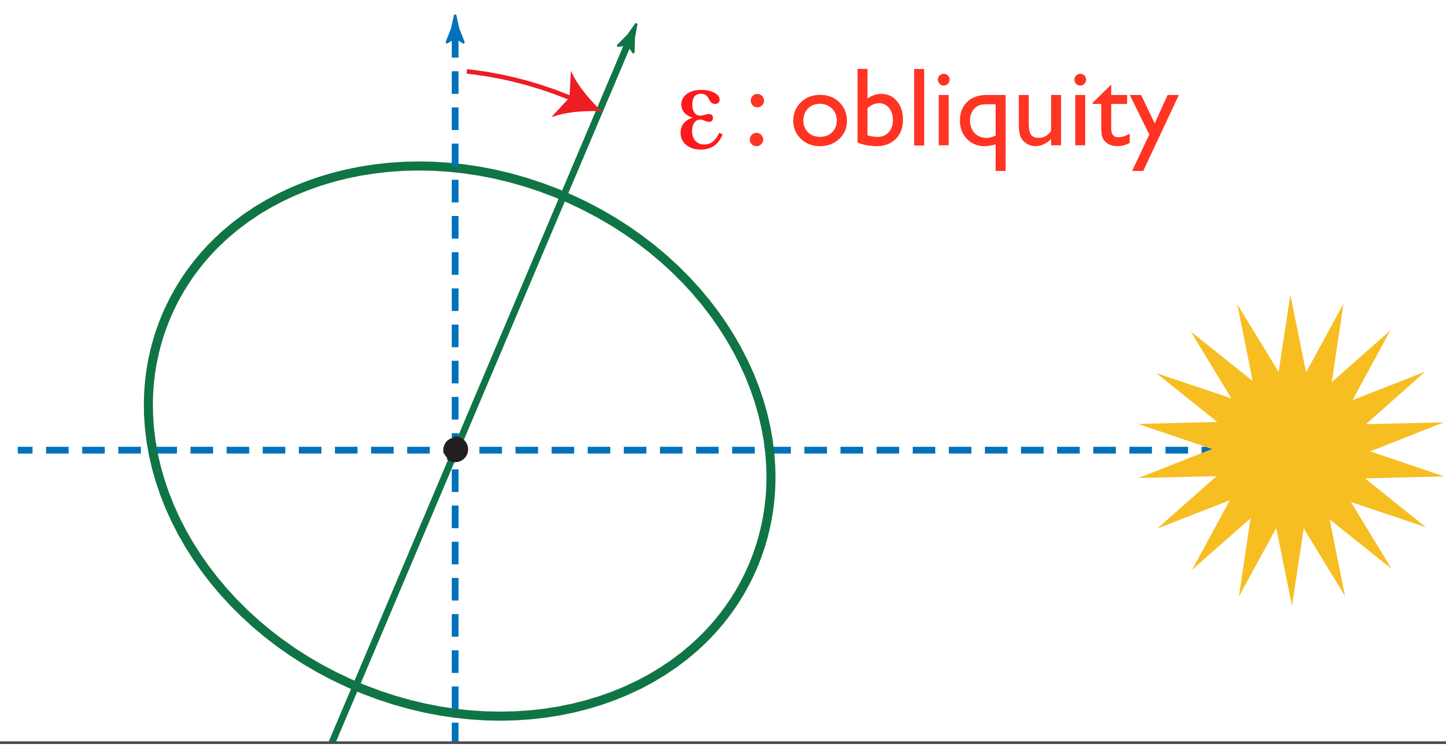

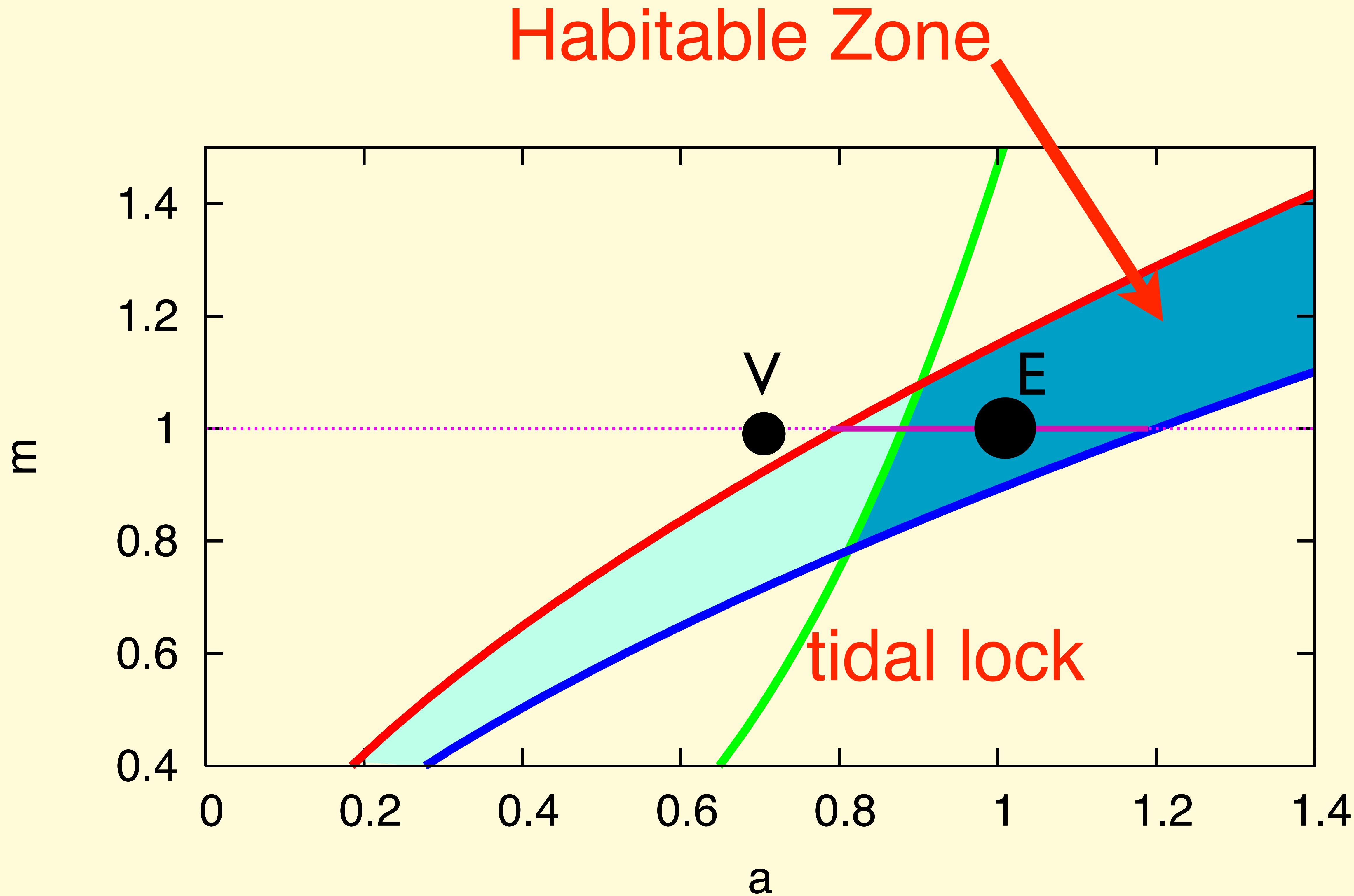
Habitable Zone
1.4
1.2
1
0.8
0.6
0.4
m
V
E
tidal lock
0
0.2
0.4
0.6
0.8
1
1.2
1.4
a

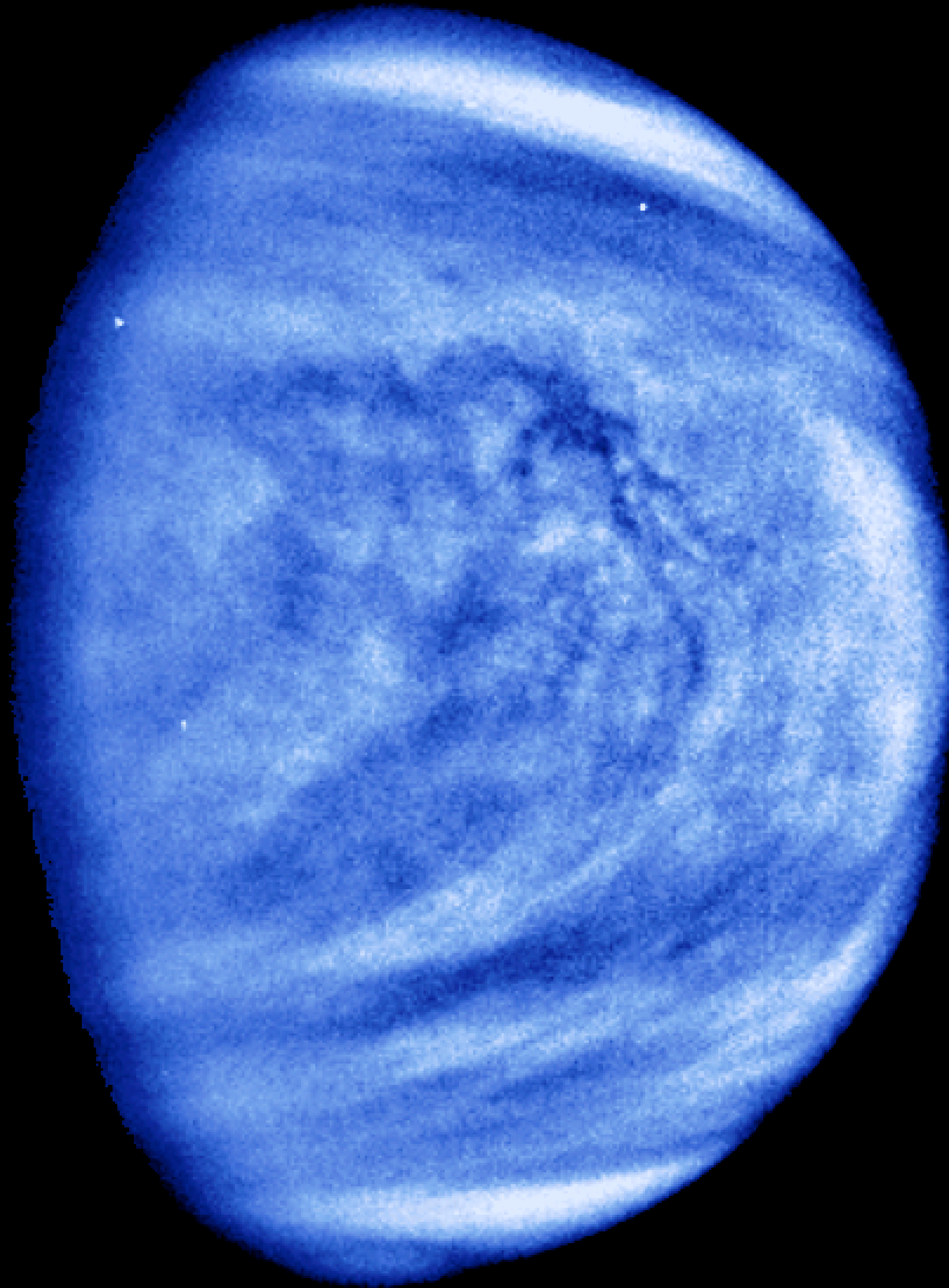

The rotation of Venus

Tidal dissipation

Darwin, 1880; Gersternkorn, 1955; Kaula, 1964; Goldreich, 1966; Mignard, 1979,80,81; Hut, 1981; Touma & Wisdom, 1994; Néron de Surgy & Laskar, 1997; Efroimsky & Williams, 2009; Ferraz-Mello, 2013; Correia, Boué, Laskar, Rodriguez, 2014;

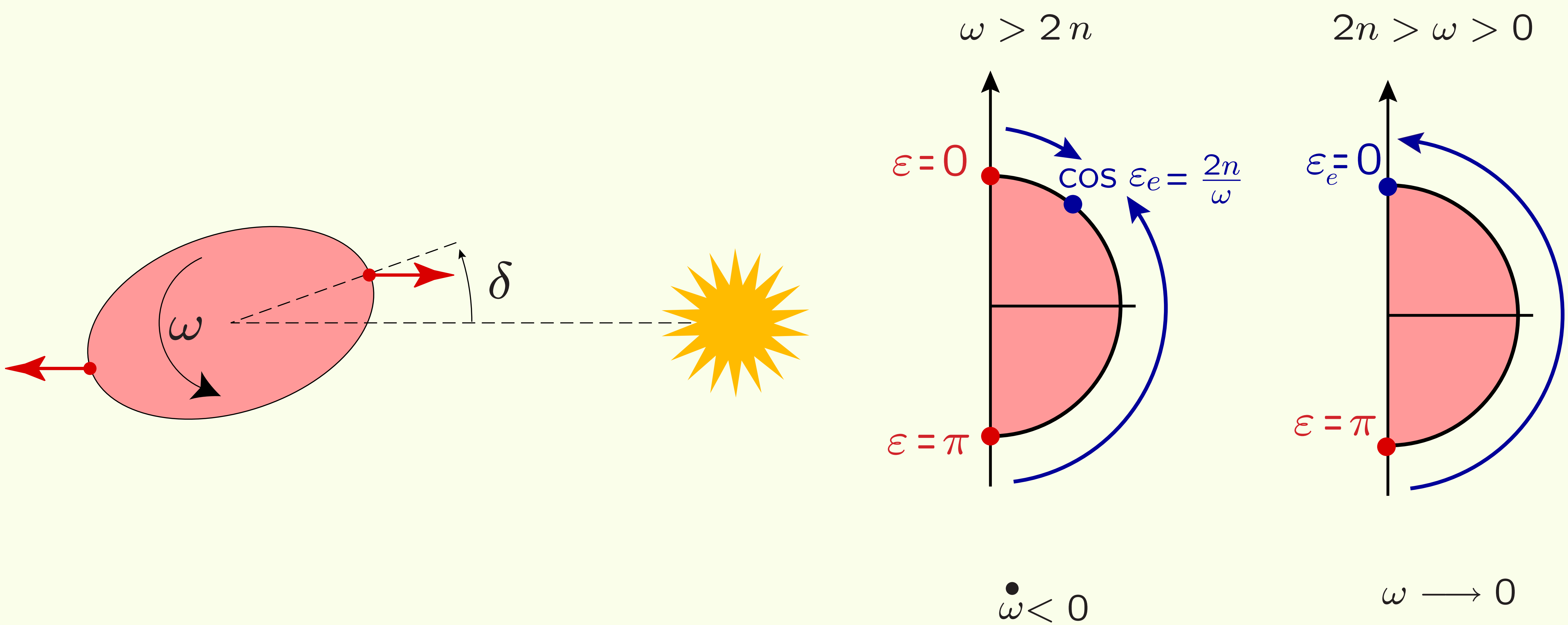

Core-mante friction

Poincaré, 1910; Greenspan & Howard, 1963; Busse, 1928; Goldreich & Peale, 1967; Roberts & Stewartson, 1975; Rochester, 1976;Dobrovolskis, 1980; Yoder, 1995; Néron de Surgy & Laskar, 1997; Païs et al., 1999

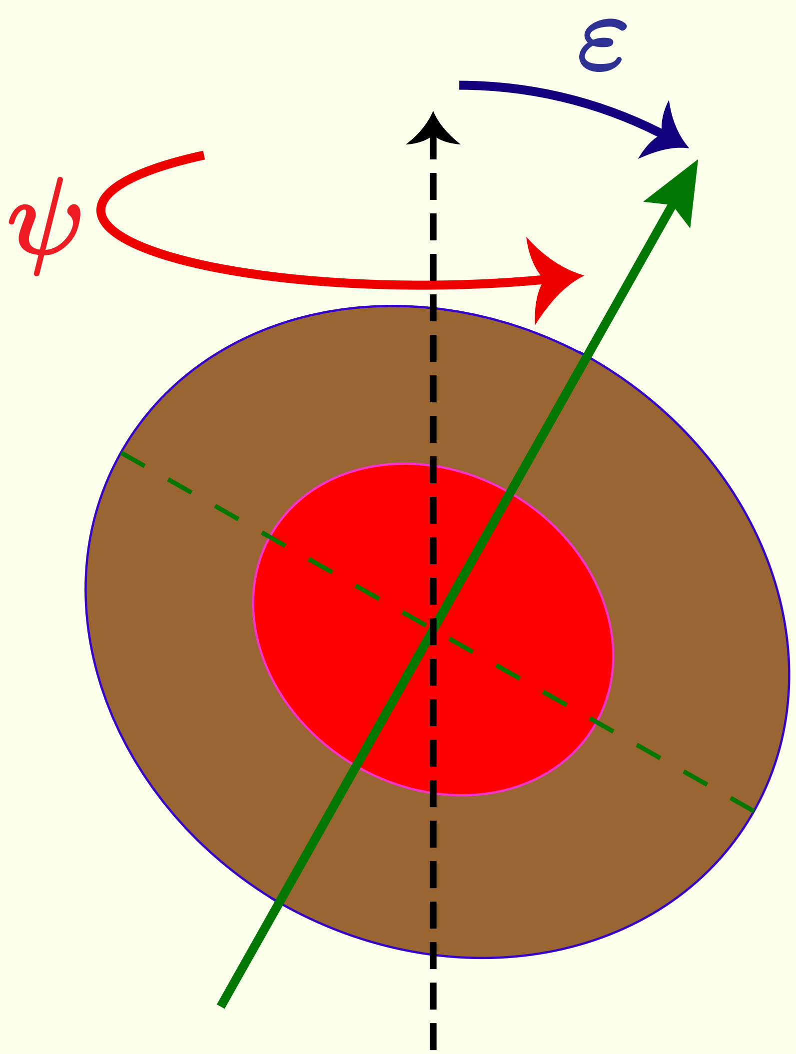

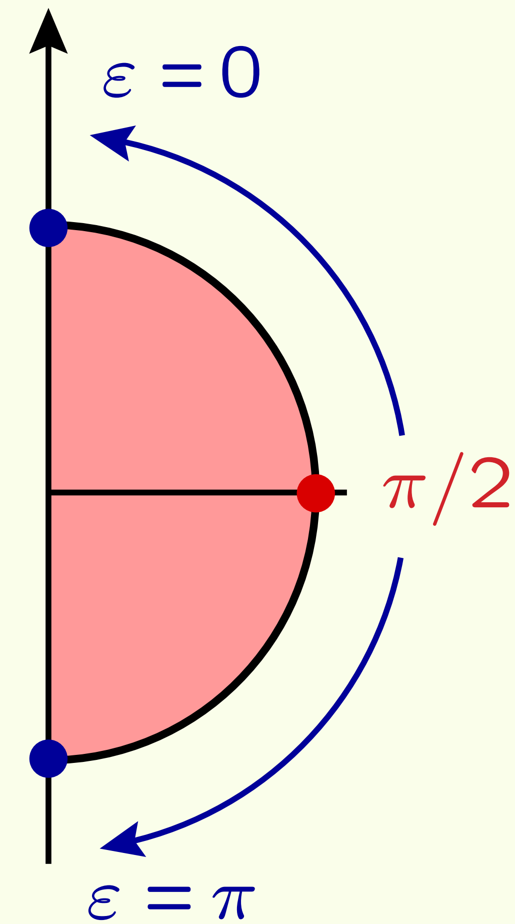

$\dot{\omega} < 0$

$10^{-7} < \nu < 10^{5}$ (Lumb & Aldridge, 1991)

Atmospheric tides

Chapman & Lindzen, 1970; Dobrovolskis & Ingersoll, 1980; Hinderer, Legros, Pedotti, 1980; Correia & Laskar, 2002

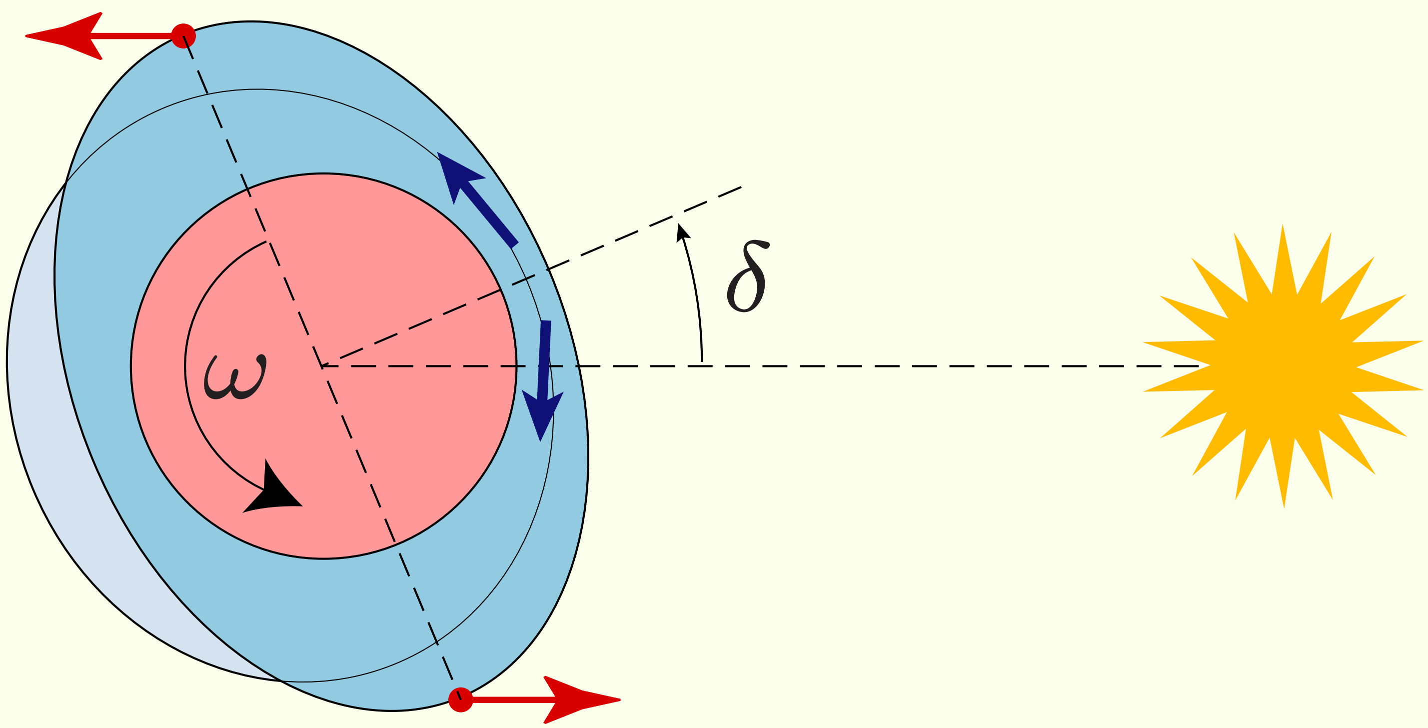

$\omega > 2\,n$

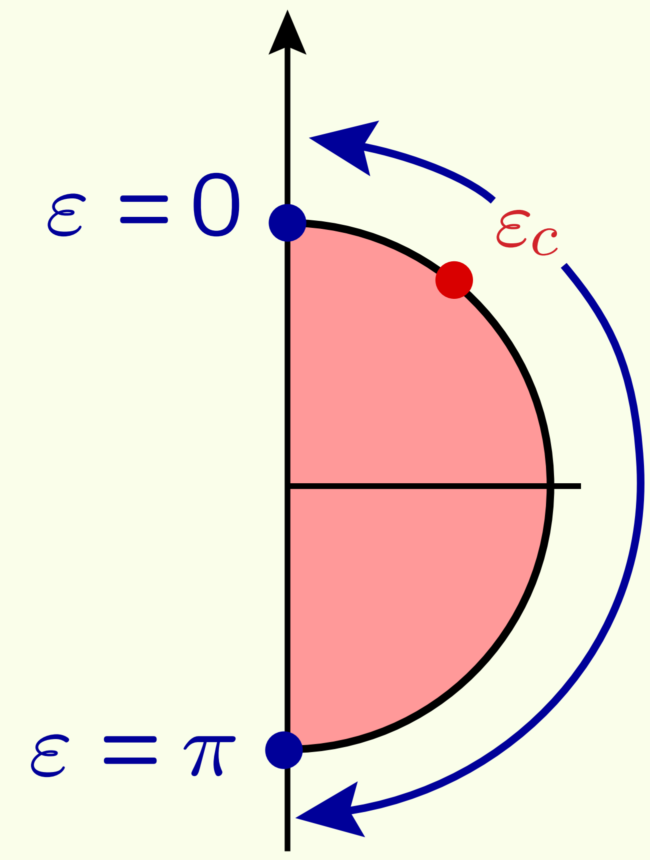

$\dot{\omega} > 0$

A back garden experiment

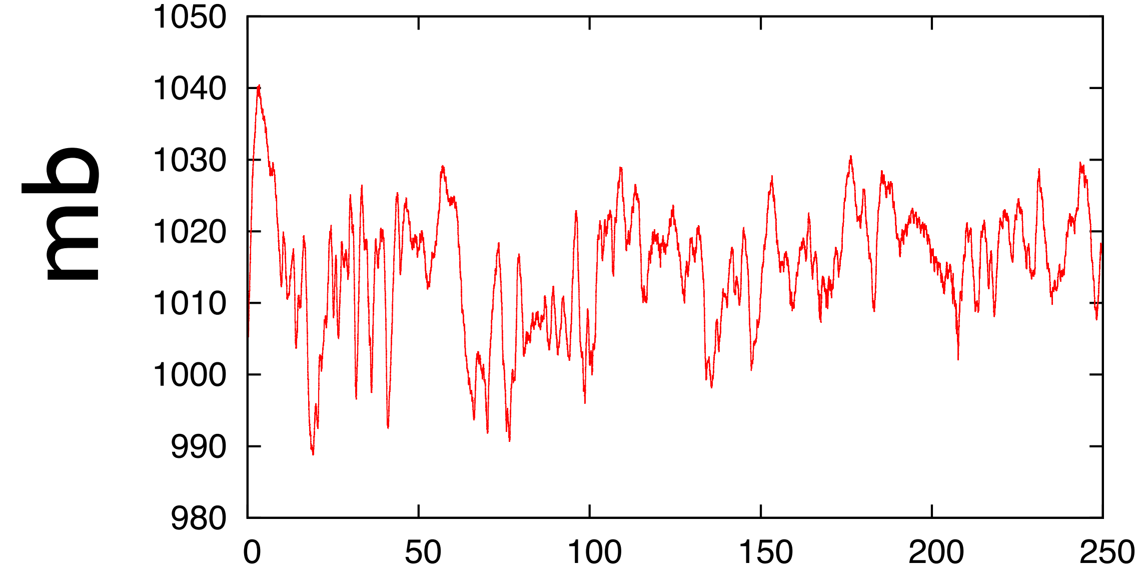

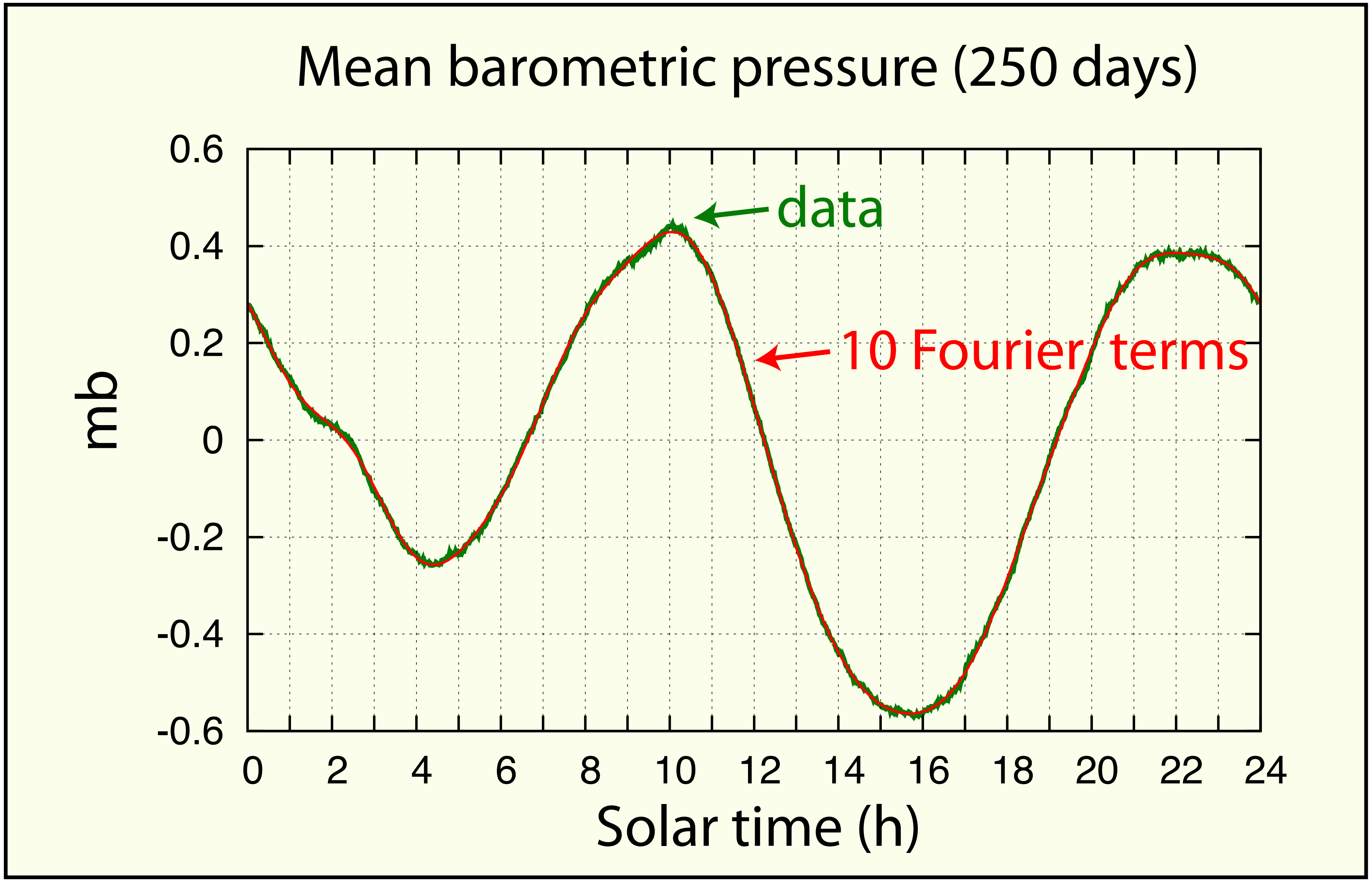

tidal friction

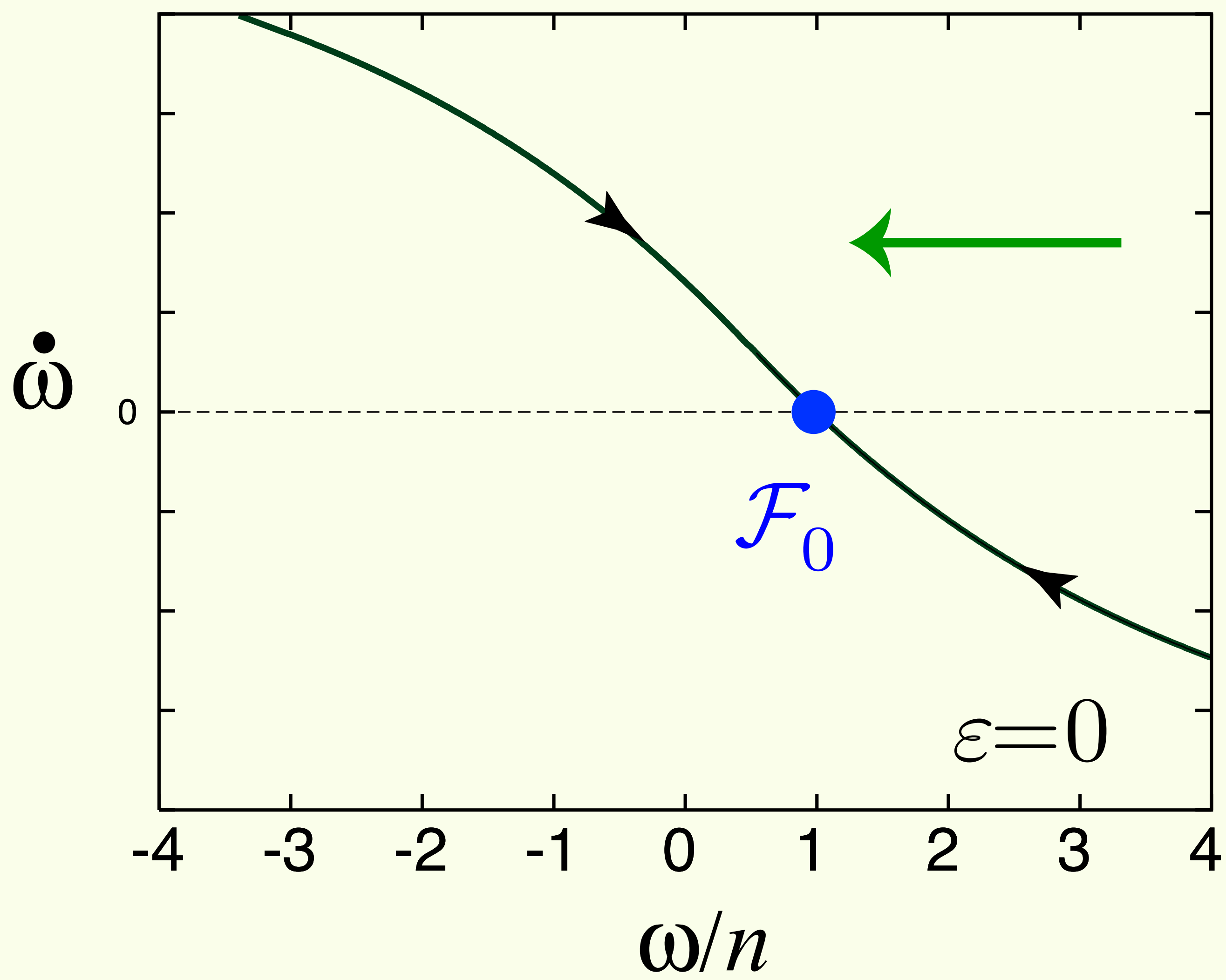

Correia & Laskar, Icarus, 2003

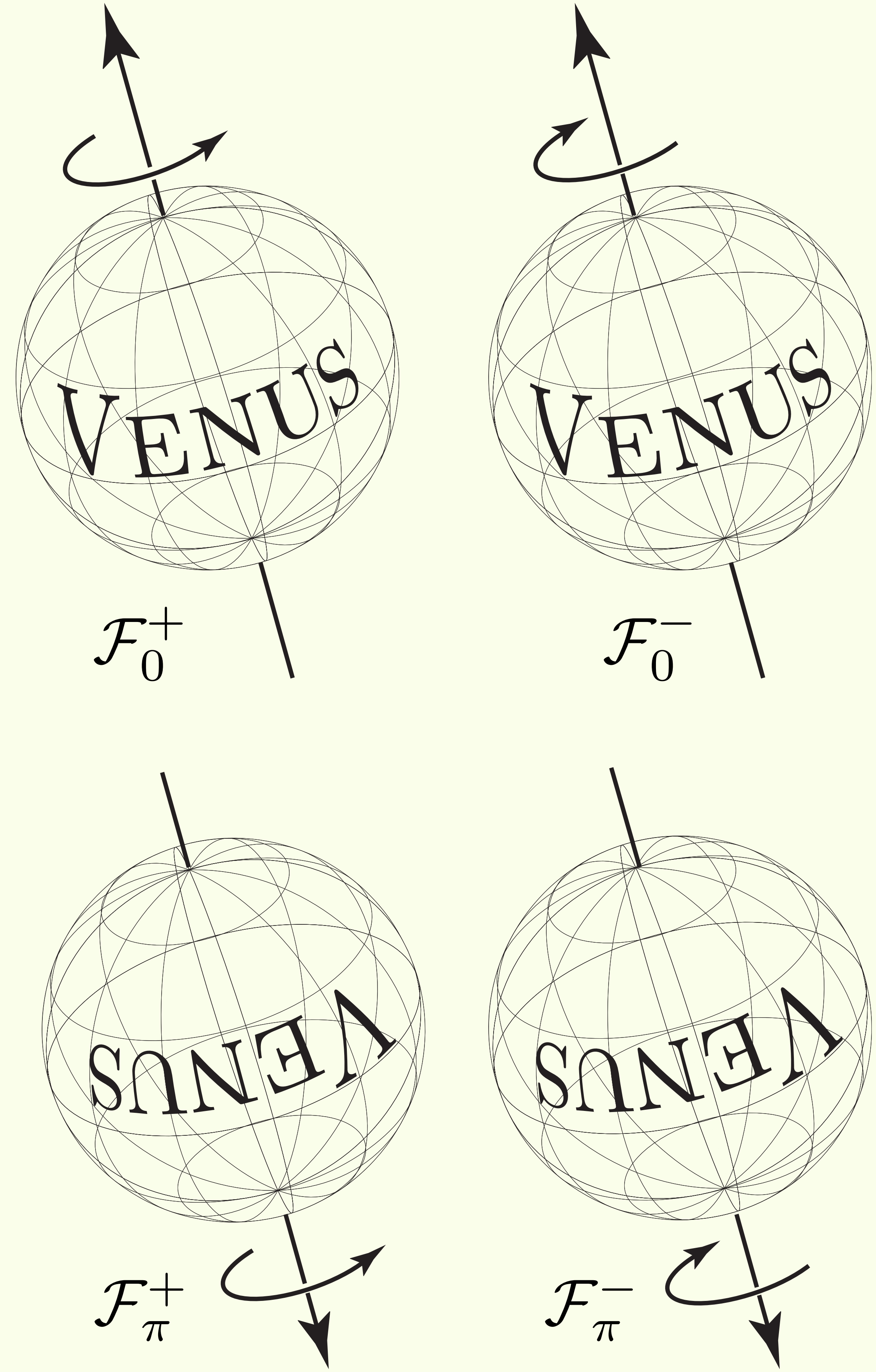

Correia & Laskar, *Nature*, 2001

Without planetary perturbations

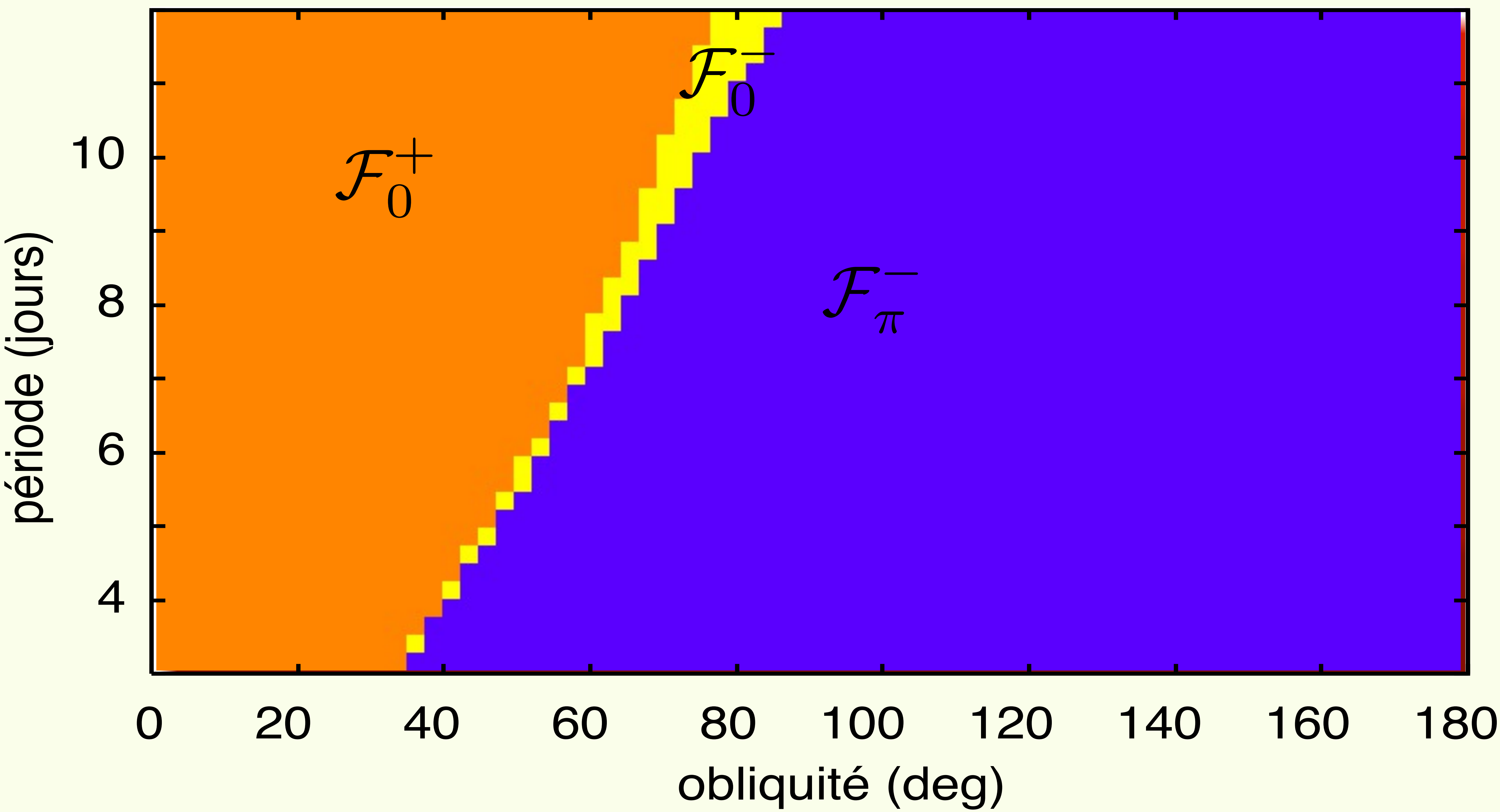

Correia & Laskar, *Nature*, 2001

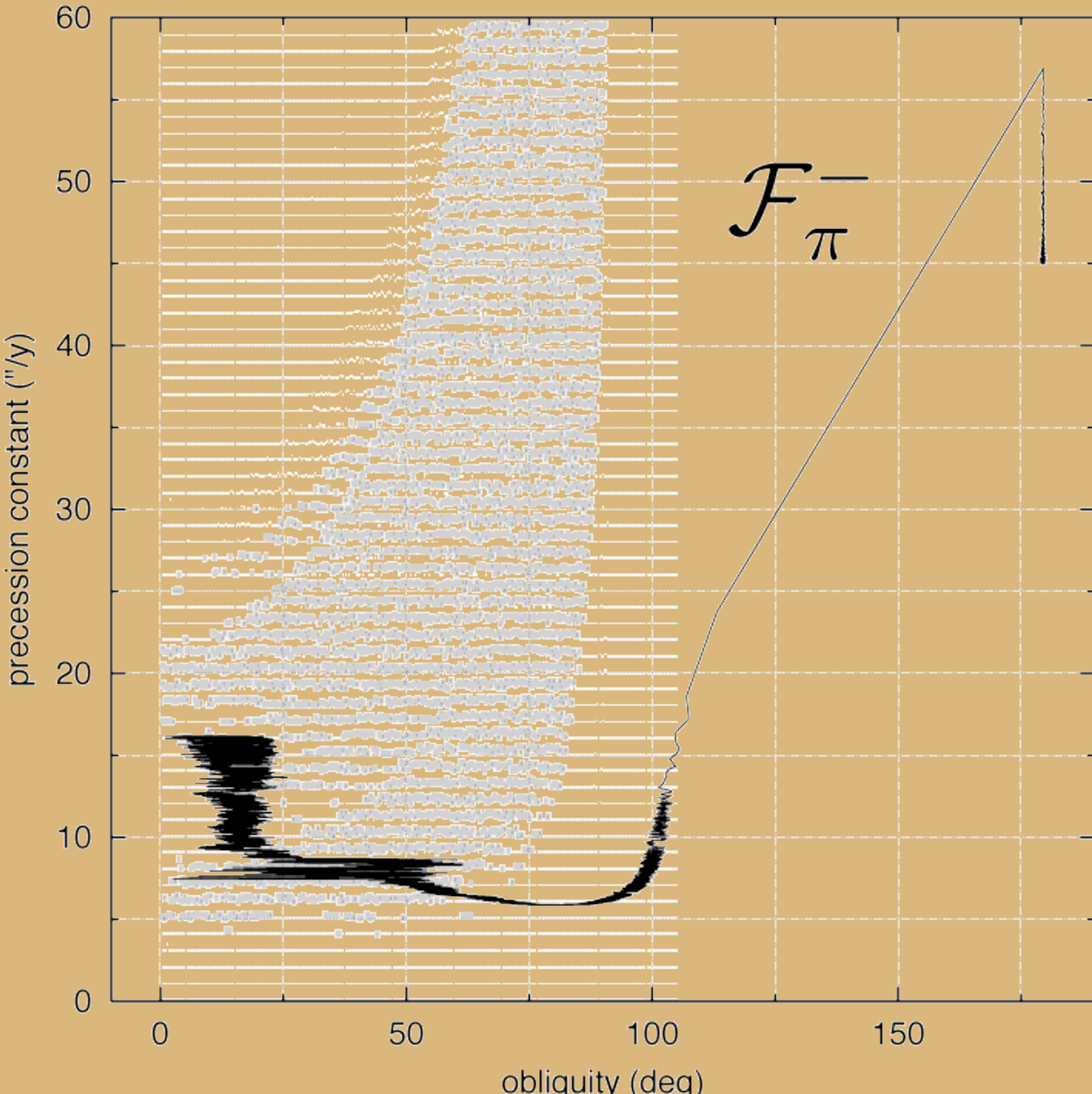

precession constant ("/y)
obliquity (deg)
$\mathcal{F}_{\pi}^{-}$
0
10
20
30
40
50
60
0
50
100
150

With planetary perturbations

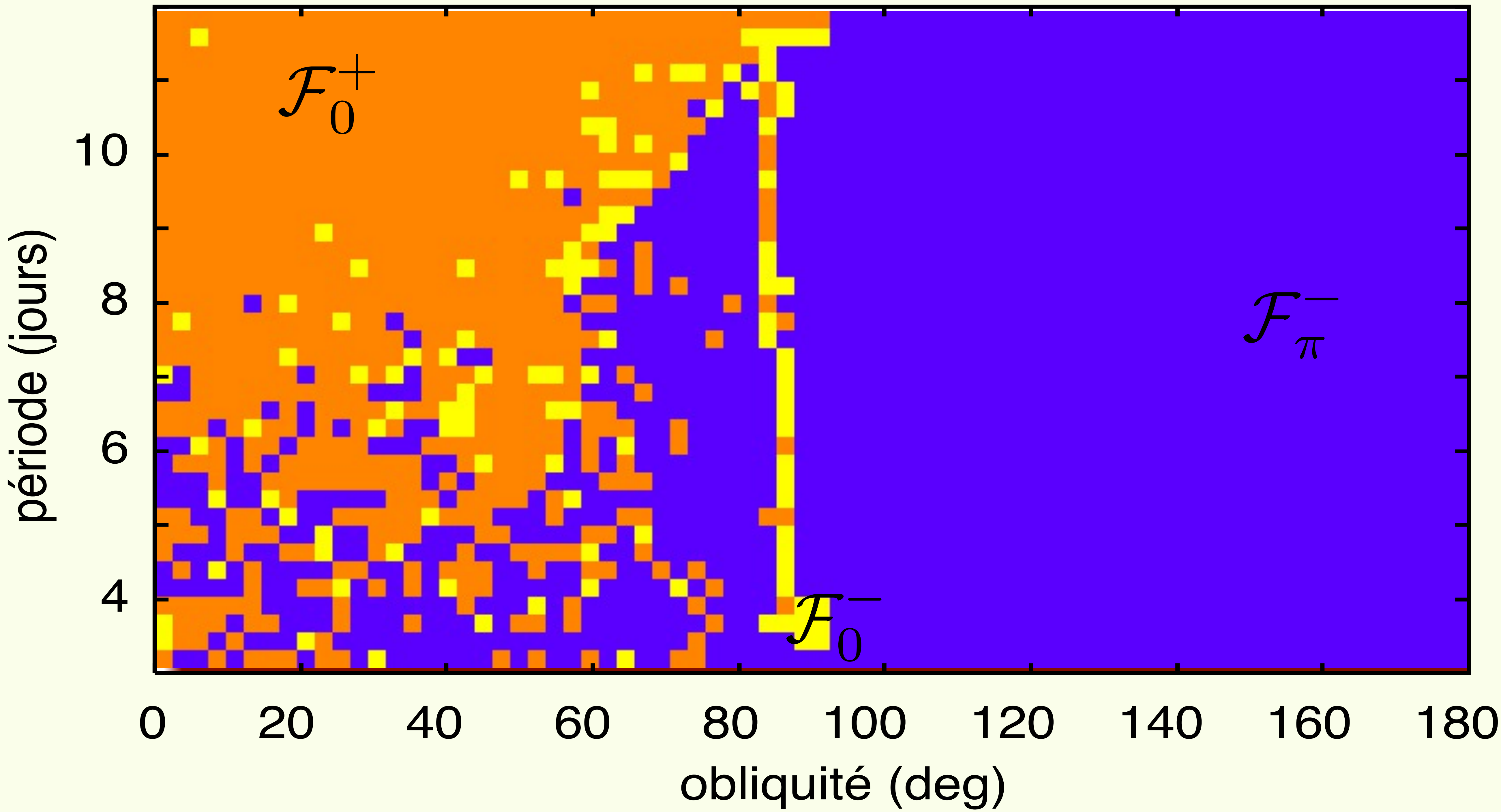

Correia & Laskar, *Nature*, 2001

Tidal dissipation

Tidal dissipation
+
atmosperic tides

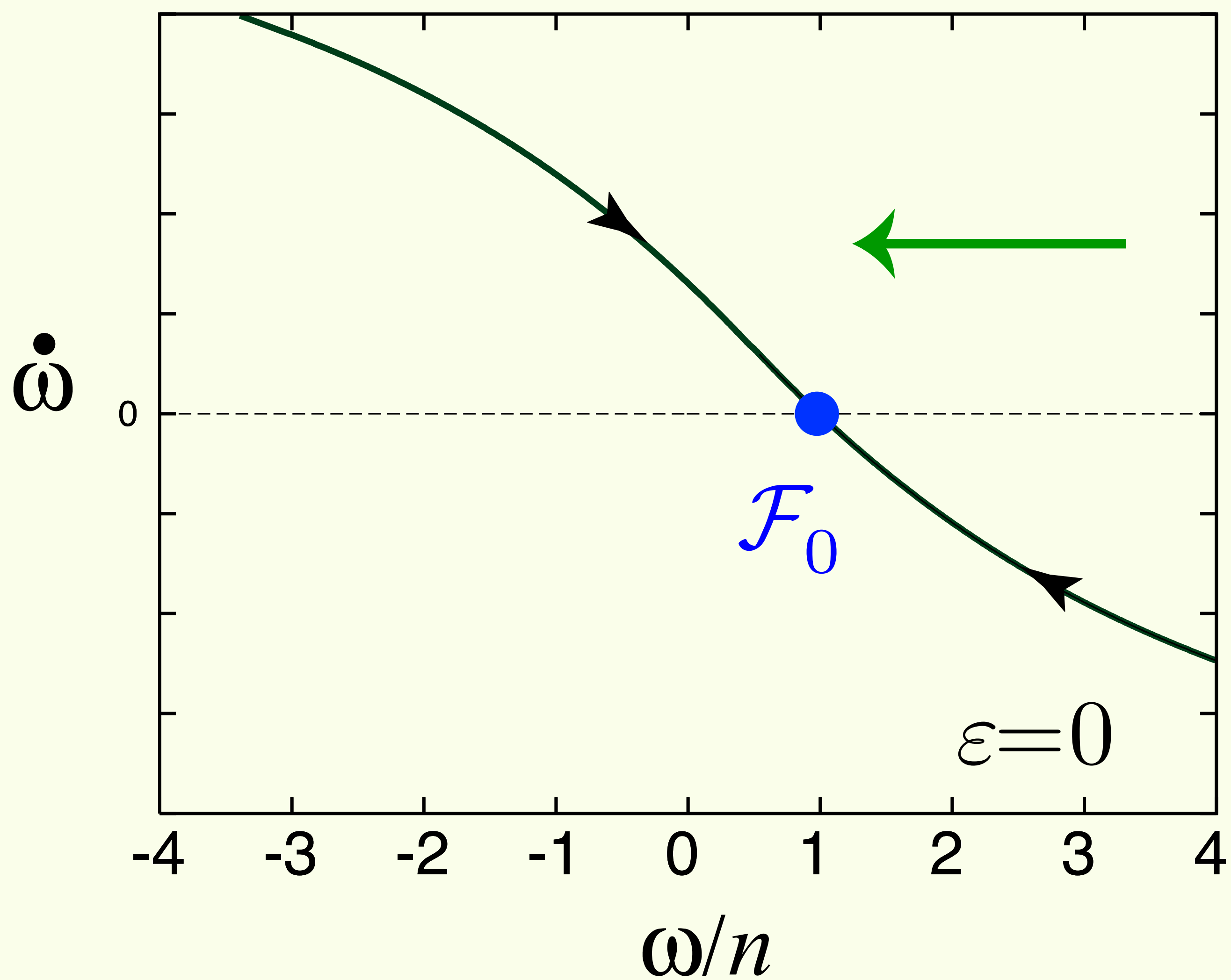

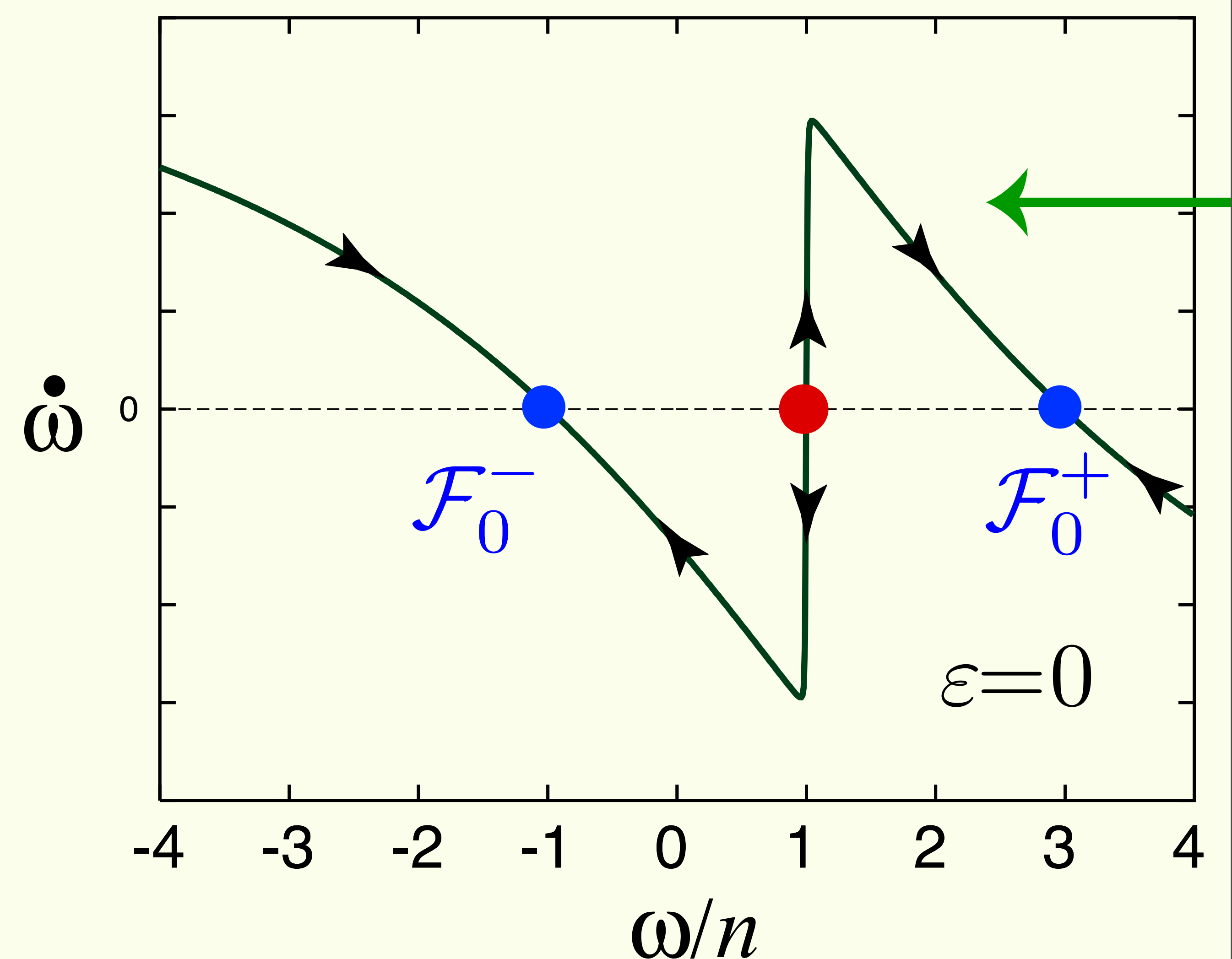

Correia & Laskar, Icarus, 2003

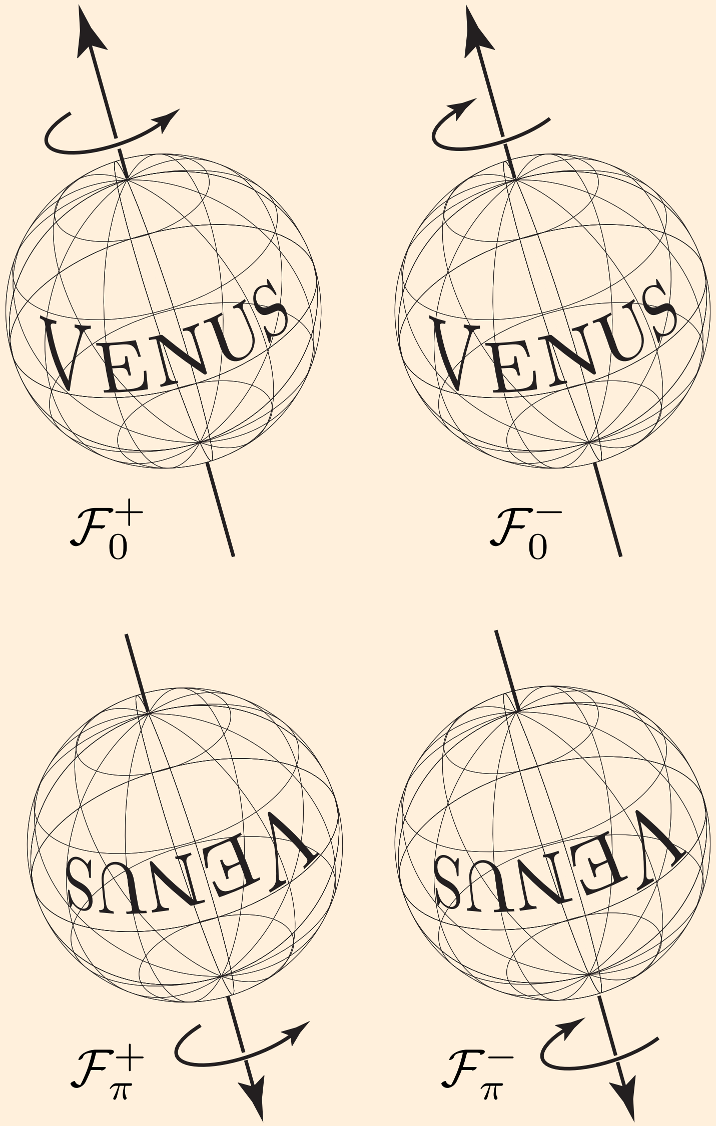

Correia & Laskar, *Nature*, 2001

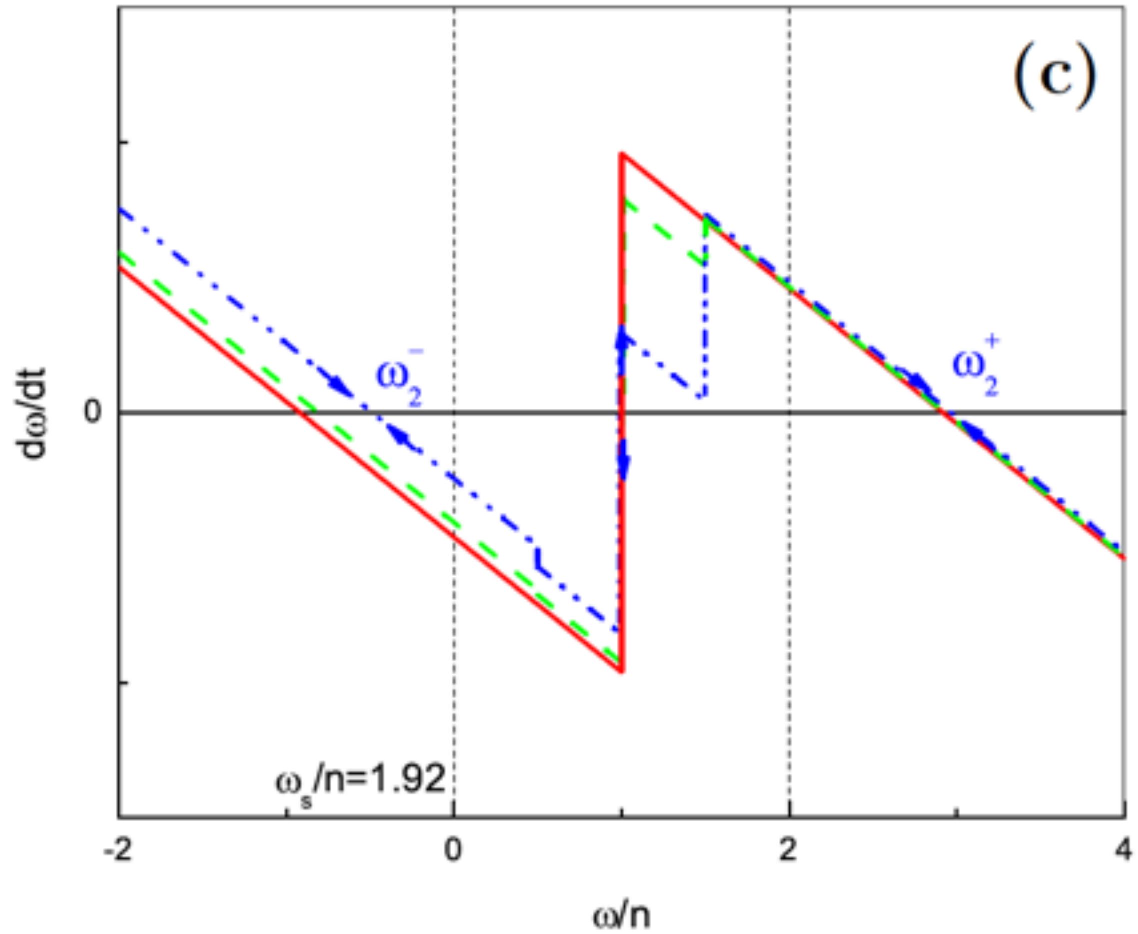

Fig. 3. Variation of $\dot{\omega}$ with ω/n (Eq. 53) for **(a)** $\omega_s/n = 0.05$, **(b)** $\omega_s/n = 0.55$, and **(c)** $\omega_s/n = 1.92$, using different eccentricities (e=0.0, 0.1, 0.2). The equilibrium rotation rates are given by $\dot{\omega} = 0$ and the arrows indicate whether it is a stable or unstable equilibrium position.

Spin evolution of Earth-sized exoplanets, including atmospheric tides and core-mantle friction

Diana Cunha[1,2], Alexandre C. M. Correia[3,4], and Jacques Laskar[4] **(2014)**

PhD Thesis of Pierre Auclair-Desrotour (S. Mathis - J. Laskar)

The 3/2 spin-orbit resonance of Mercury

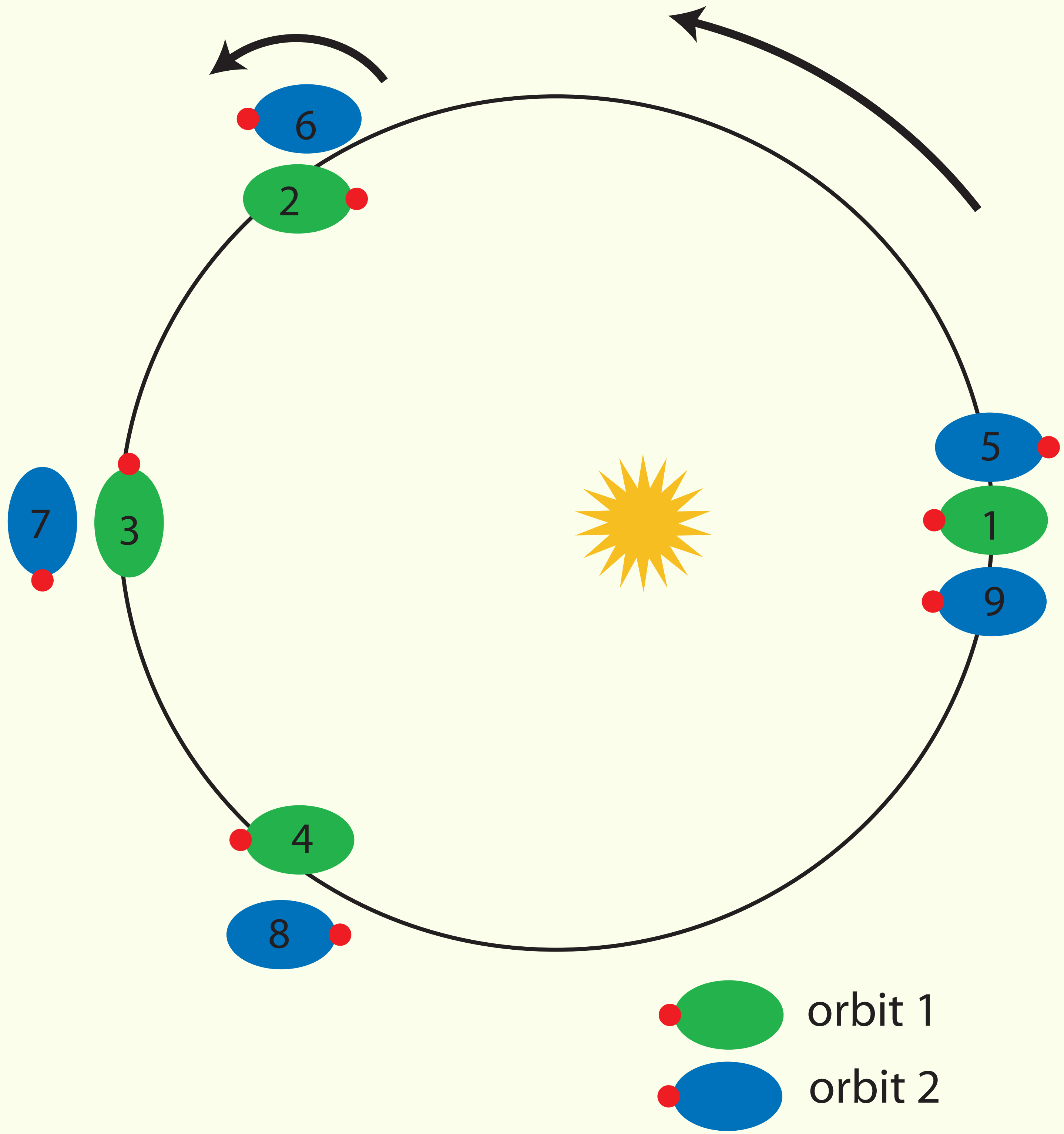

3/2 resonance

Rotation Period : 58.6 d
Orbital Period : 87.97d

Radar observations:
Pettengill & Dyce, 1965

Peale & Gold, 1965
Goldreich, 1965
Colombo, 1965
Liu & O'Keefe, 1965
Goldreich & Peale, 1966
Counselman & Shapiro, 1970

Tidal dissipation

Peale & Gold, 1965, Goldreich, 1965, Goldreich & Peale, 1966

$$\dot{x} = -K\left[\Omega(e)x - N(e)\right] \qquad x = \dot{\ell}/n$$

$$x_l(e) = \frac{N(e)}{\Omega(e)} = \frac{1 + 15e^2/2 + 45e^4/8 + 5e^6/16}{(1 + 3e^2 + 3e^4/8)/(1-e^2)^{3/2}}$$

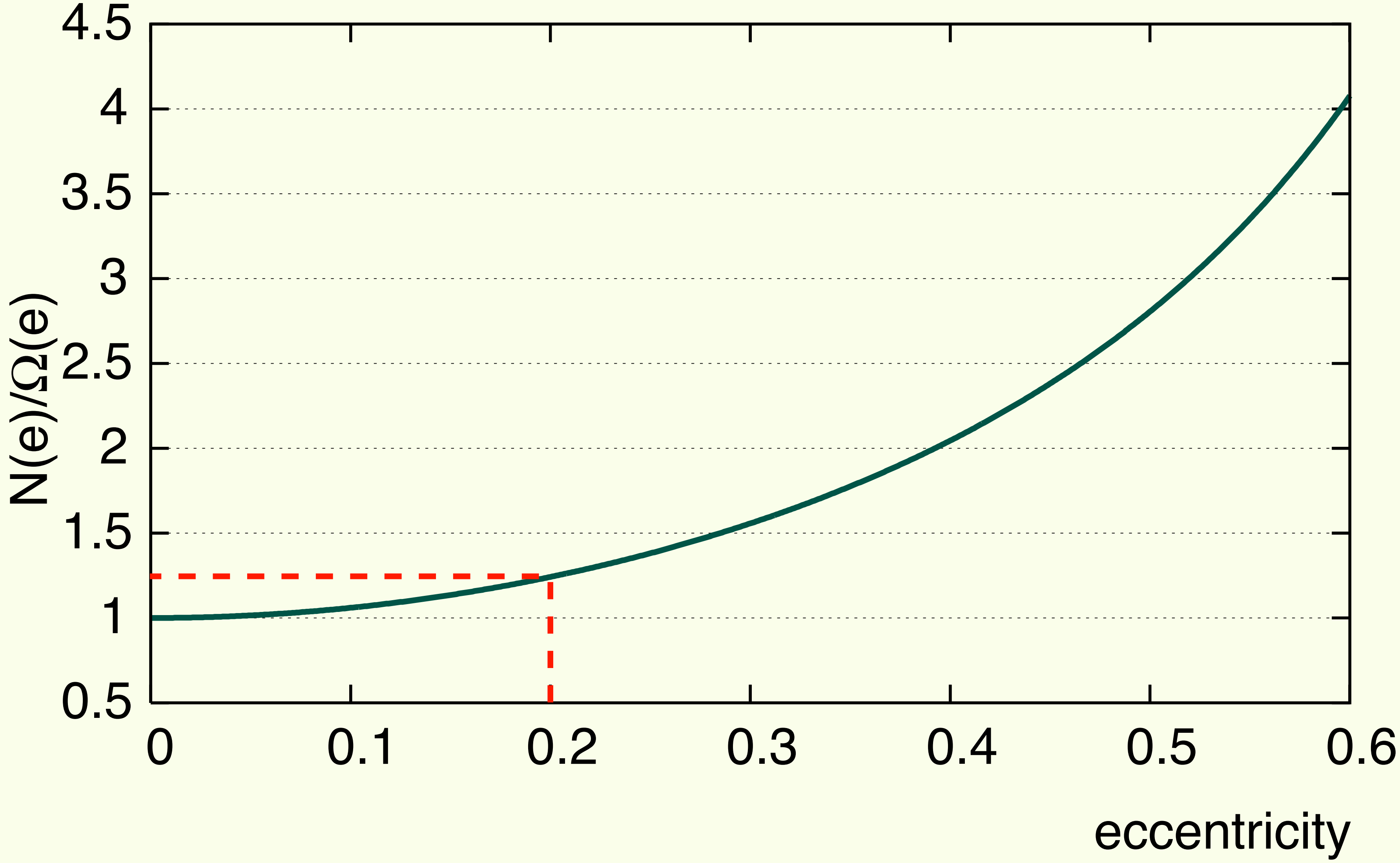

Capture Probability (%)

	G&P66 e=0.206
4/1	0,1
7/2	0,1
3/1	0,3
5/2	0,7
2/1	1,8
3/2	7,7
1/1	-
-	-

Capture Probability (%)

	G&P66 e=0.206	G&P67 e=0.206 + CMF
4/1	0,1	4,7
7/2	0,1	10,3
3/1	0,3	19,0
5/2	0,7	29,8
2/1	1,8	34,6
3/2	7,7	-
1/1	-	-
-	-	-

eccentricity distribution : chaotic solution

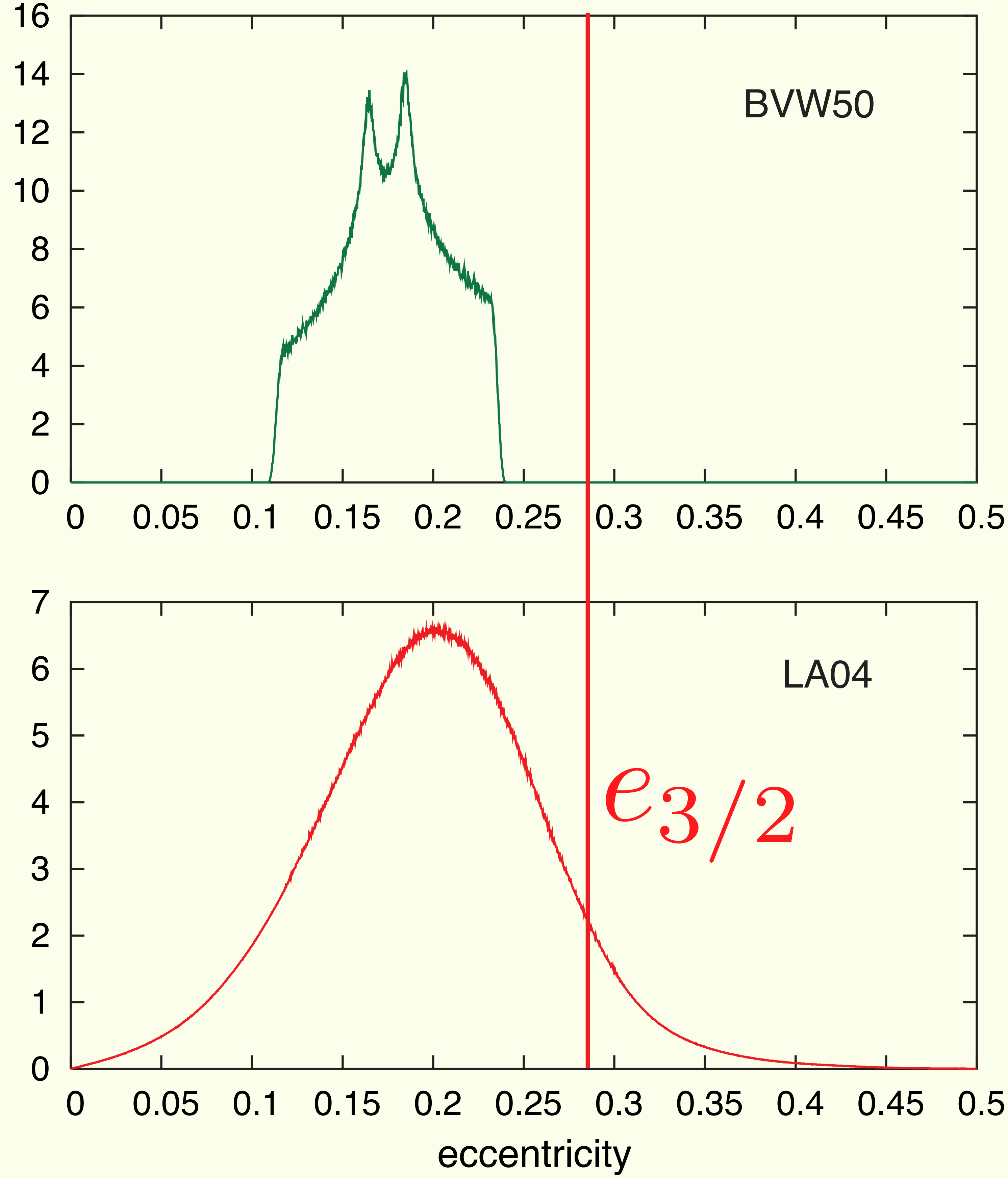

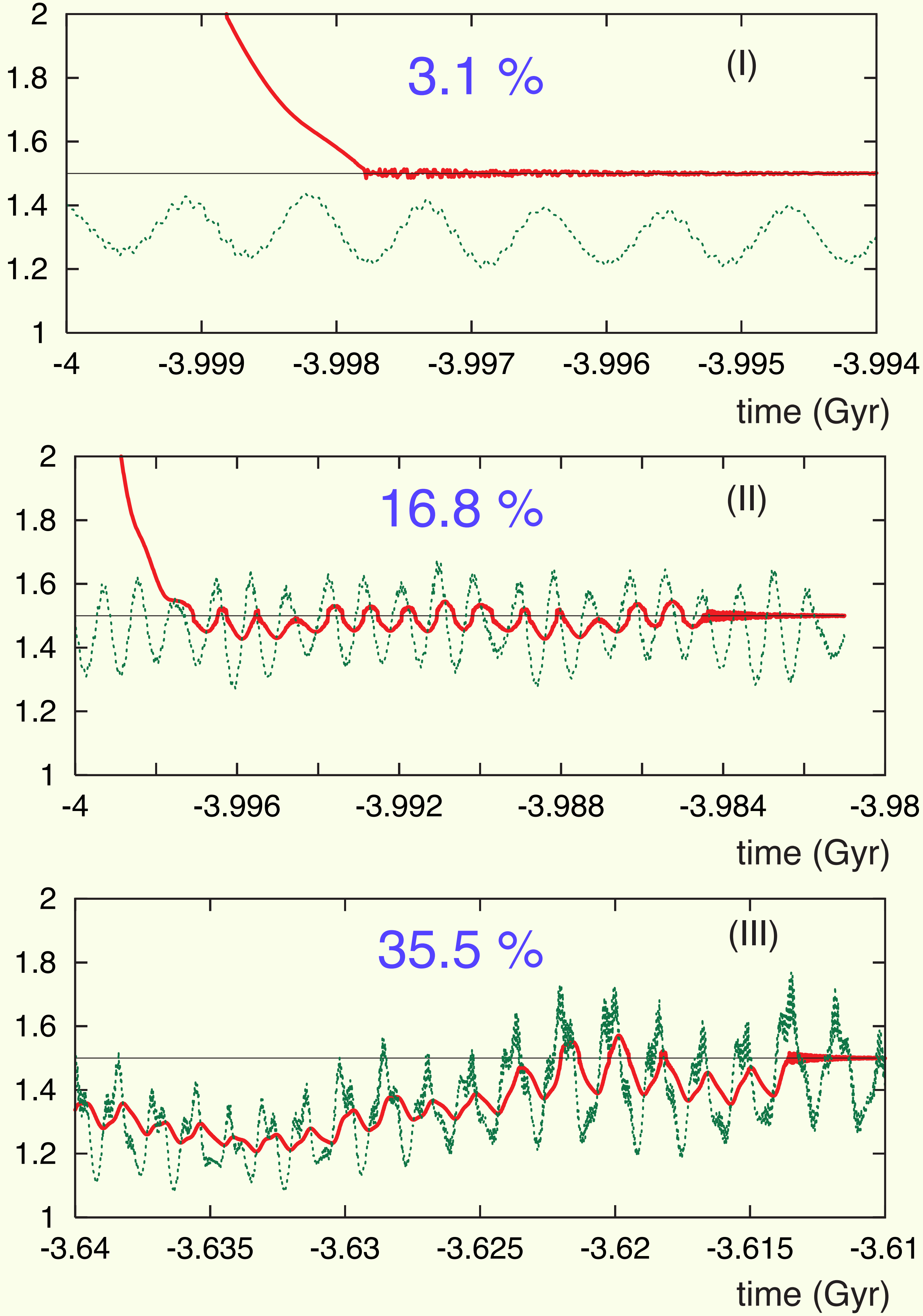

$$P_{1/1} = 2.2\%$$

$$P_{3/2} = 55.4\%$$

$$P_{2/1} = 3.6\%$$

Correia & Laskar, *Nature*, 2004

Capture Probability (%)

	G&P66 e=0.206	G&P67 e=0.206 + CMF	C&L04 chaotic e
4/1	0,1	4,7	-
7/2	0,1	10,3	-
3/1	0,3	19,0	-
5/2	0,7	29,8	-
2/1	1,8	34,6	3,6
3/2	7,7	-	55,4
1/1	-	-	2,2
-	-	-	38,3

Critical eccentricity

p	$e_c(p)$
$1/1$	$-$
$3/2$	0.000026
$2/1$	0.004602
$5/2$	0.024877
$3/1$	0.057675
$7/2$	0.095959
$4/1$	0.135506
$9/2$	0.174269
$5/1$	0.211334

The resonance p is unstable if

$$e \; < \; e_c(p)$$

Capture Probability (%)

	G&P66 e=0.206	G&P67 e=0.206 + CMF	C&L04 chaotic e	C&L08 chaotic e +CMF
4/1	0,1	4,7	-	
7/2	0,1	10,3	-	4,7
3/1	0,3	19,0	-	11,6
5/2	0,7	29,8	-	22,1
2/1	1,8	34,6	3,6	31,6
3/2	7,7	-	55,4	25,9
1/1	-	-	2,2	3,9
-	-	-	38,3	0,2

Tidal Dissipation in

Extra Solar

Planetary Systems

Kepler near-resonant planets

- Significant excess of planet pairs just exterior to MMR

Lissauer et al. (2011), Fabrycky et al. (2012)

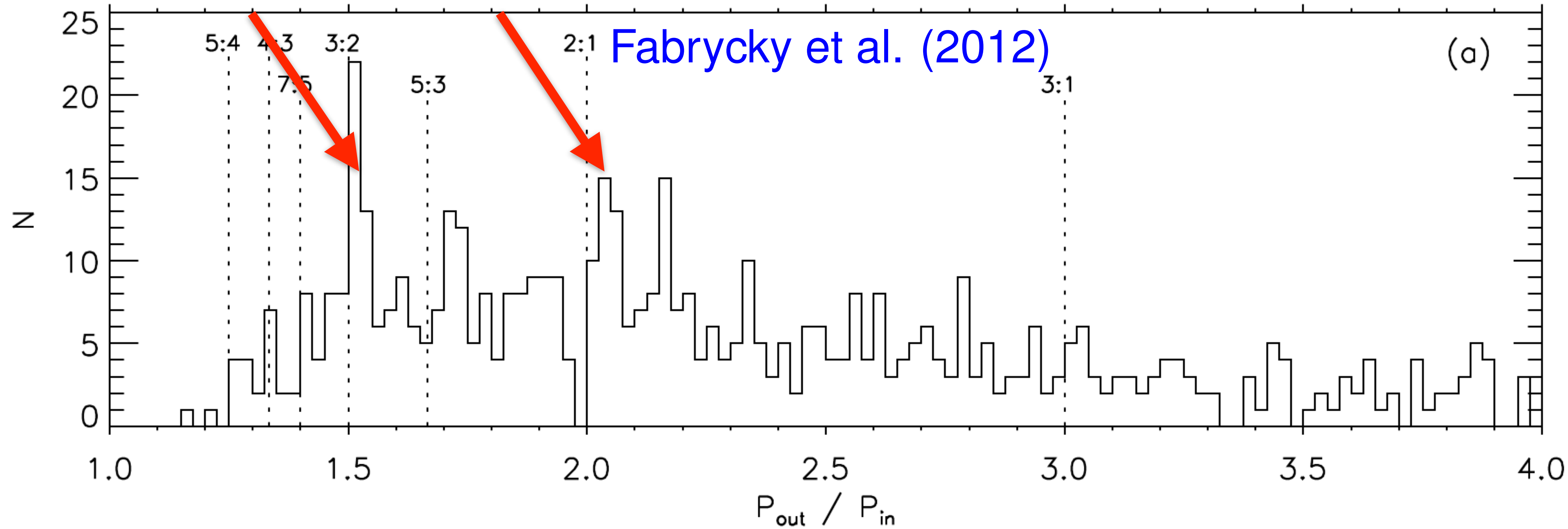

- Possibly due to dissipation (tidal effect, disk-planet interactions)

Papaloizou & Terquem (2010),
Lithwick & Wu (2012), Batygin & Morbidelli (2013),
Baruteau & Papaloizou (2013)

Delisle, Laskar, Correia, Boué, (2012), Lee, Fabrycky, Lin (2013)

2 DOF (4 dimensional phase space) + 1 const (G).

- Resonant averaged Hamiltonian (p+q:p) (*lower deg*)

Kepler secular resonant

$$\mathcal{H} = \mathcal{K}(\mathcal{D}) + \mathcal{S}_q(I_i, \Delta\varpi) + \sum_{k=0}^{q} R_k (x_1^k x_2^{q-k} + \bar{x}_1^k \bar{x}_2^{q-k})$$

deg ≥ 2 deg = q

- Long term evolution of G :

$$\begin{aligned} \left.\frac{\mathrm{d}G}{\mathrm{d}t}\right|_{\mathrm{d}} = & -\Lambda_1 \frac{e_1^2}{\sqrt{1-e_1^2}} \left.\left(\frac{\dot{e}_1}{e_1}\right)\right|_{\mathrm{d}} \\ & -\Lambda_2 \frac{e_2^2}{\sqrt{1-e_2^2}} \left.\left(\frac{\dot{e}_2}{e_2}\right)\right|_{\mathrm{d}} \\ & +\frac{1}{2}\Lambda_1\Lambda_2 \left(\sqrt{1-e_1^2} - \left(1+\frac{q}{p}\right)\sqrt{1-e_2^2}\right) \left.\left(\frac{\dot{\alpha}}{\alpha}\right)\right|_{\mathrm{d}} \end{aligned}$$

Delisle, Laskar, Correia, Boué, 2012

Dissipative case: simulation

- Convergent migration (gray dots)
- Locking into 3 : 2 MMR
- Tidal damping (black dots)

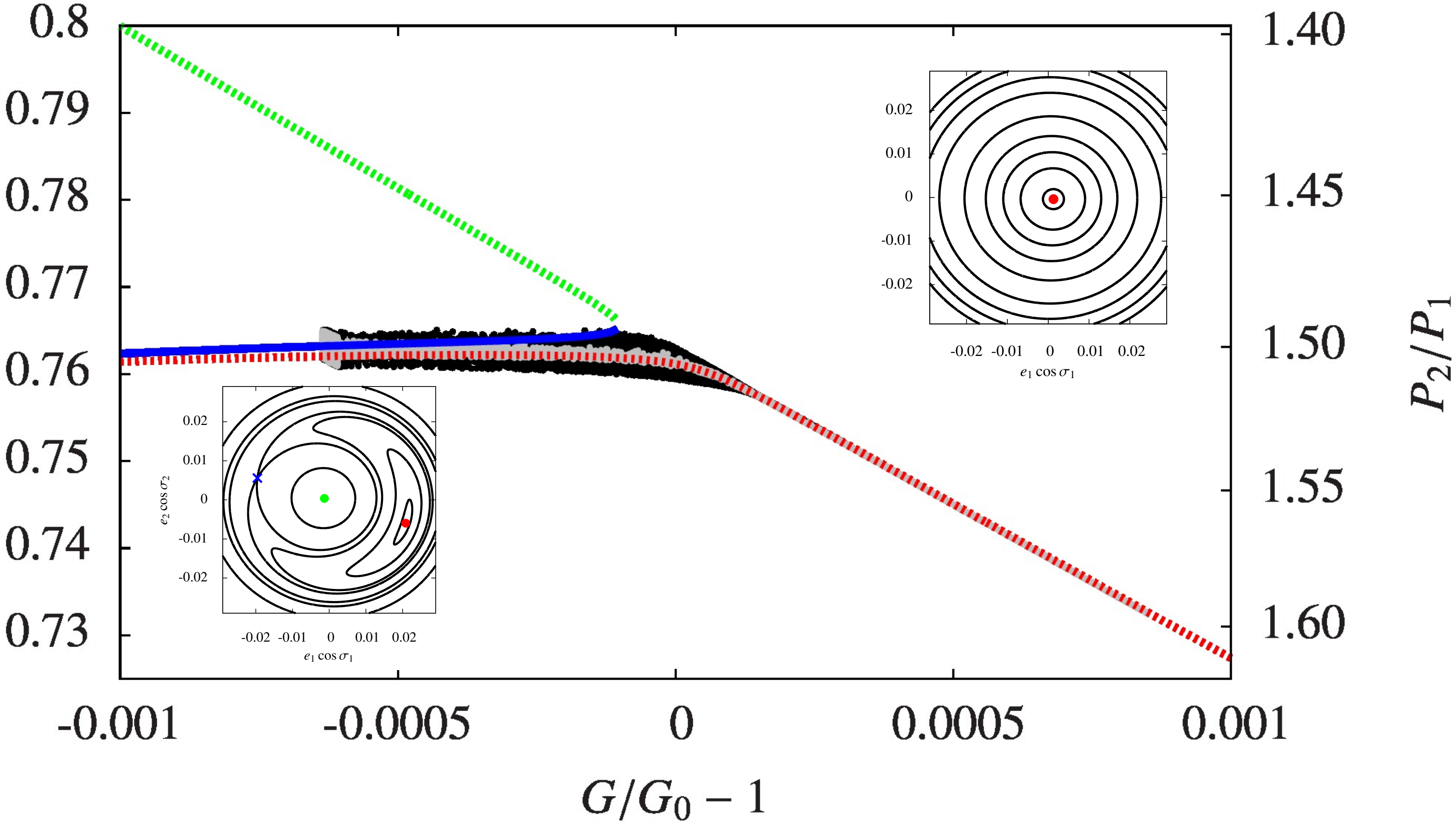

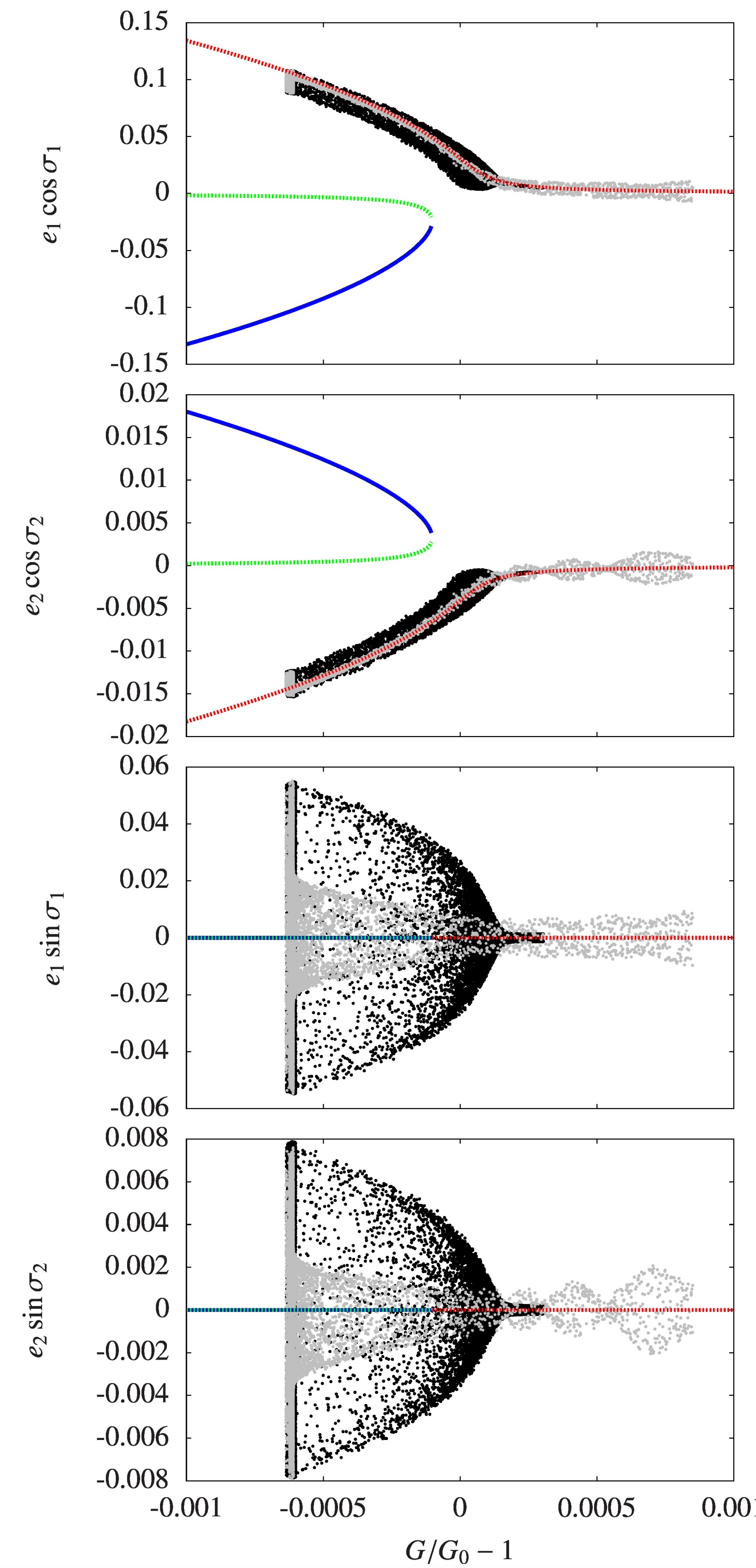

(Delisle, Laskar, Correia, Boué, 2012)

Higher order MMR (p+q:p) q > 1

- Resonant averaged Hamiltonian (p+q:p) (*lower deg*)

Kepler secular resonant

$$\mathcal{H} = \mathcal{K}(\mathcal{D}) + \mathcal{S}_q(I_i, \Delta\varpi) + \sum_{k=0}^{q} R_k(x_1^k x_2^{q-k} + \bar{x}_1^k \bar{x}_2^{q-k})$$

deg ≥ 2 deg = q

Higher order MMR (p+q:p) q > 1

- Search for the center of libration :

$$\dot{x}_i = \boldsymbol{i}\frac{\partial \mathcal{H}}{\partial \bar{x}_i} = 0$$

$$I_{i,ell},\ \sigma_{i,ell}$$

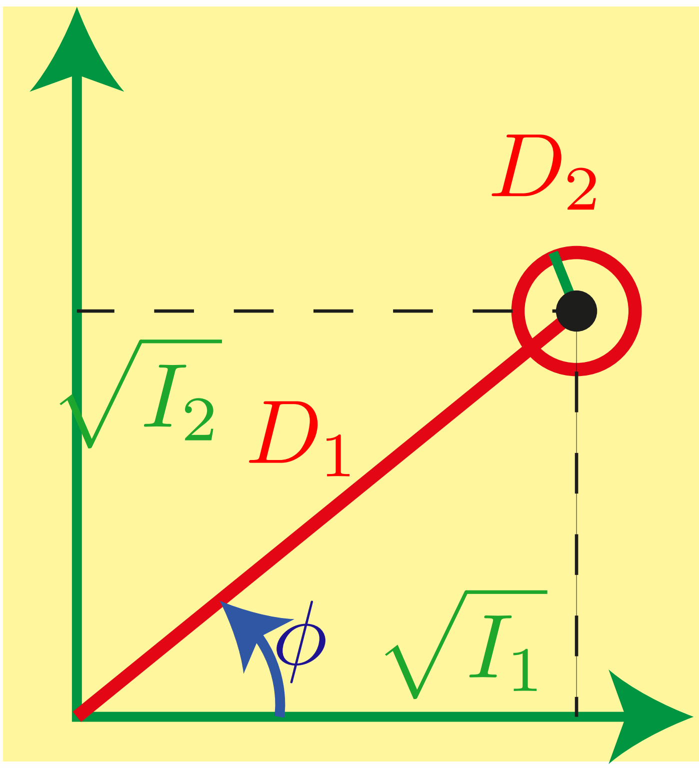

$$\tan\phi = \sqrt{\frac{I_{2,ell}}{I_{1,ell}}}$$

$$x = M_\sigma R_\phi u$$

$$(M_\sigma)_{i,i} = \boldsymbol{e}^{\boldsymbol{i}\sigma_{i,ell}}$$

$$u_i = \sqrt{D_i}\boldsymbol{e}^{\boldsymbol{i}\theta_i}$$

$$\mathcal{H} = \mathcal{K}(\mathcal{D}) + \mathcal{S}'_q(D_i, \theta_2 - \theta_1) + \sum_{k=0}^{q} R'_k(u_1^k u_2^{q-k} + \bar{u}_1^k \bar{u}_2^{q-k})$$

$$\mathcal{D} = D_1 + D_2 = u_1\bar{u}_1 + u_2\bar{u}_2$$

Delisle, Laskar, Correia, 2014

Separatrix crossing. Final outcome

$$\tau_c \approx L \left(\frac{e_1}{e_2}\right)^2 \frac{4 + (p+q)(1+L)}{4L - p(1+L)}$$

$$\tau_\alpha \approx \frac{e_1^2}{e_2^2}$$

$$\tau = \frac{T_1}{T_2}$$

$$L \approx \frac{m_1}{m_2}\left(\frac{p}{p+q}\right)^{1/3}$$

$\tau < \tau_c$

- libration amplitude increases
- separatrix crossing is possible
  - ⋆ $\tau < \tau_\alpha$ Diverging $P_2/P_1 > p + q/p$
  - ⋆ $\tau > \tau_\alpha$ Converging $P_2/P_1 < p + q/p$

$\tau > \tau_c$

- libration amplitude decreases
  - ⋆ q=1 : Diverging $P_2/P_1 > p + q/p$
  - ⋆ q>1 : Stays in resonance

Delisle, Laskar, Correia, 2014

GJ163 b : gaz
GJ163 c : rock

GJ163 b,c 3:1 MMR

$$\frac{P_c}{P_b} = 2.97$$

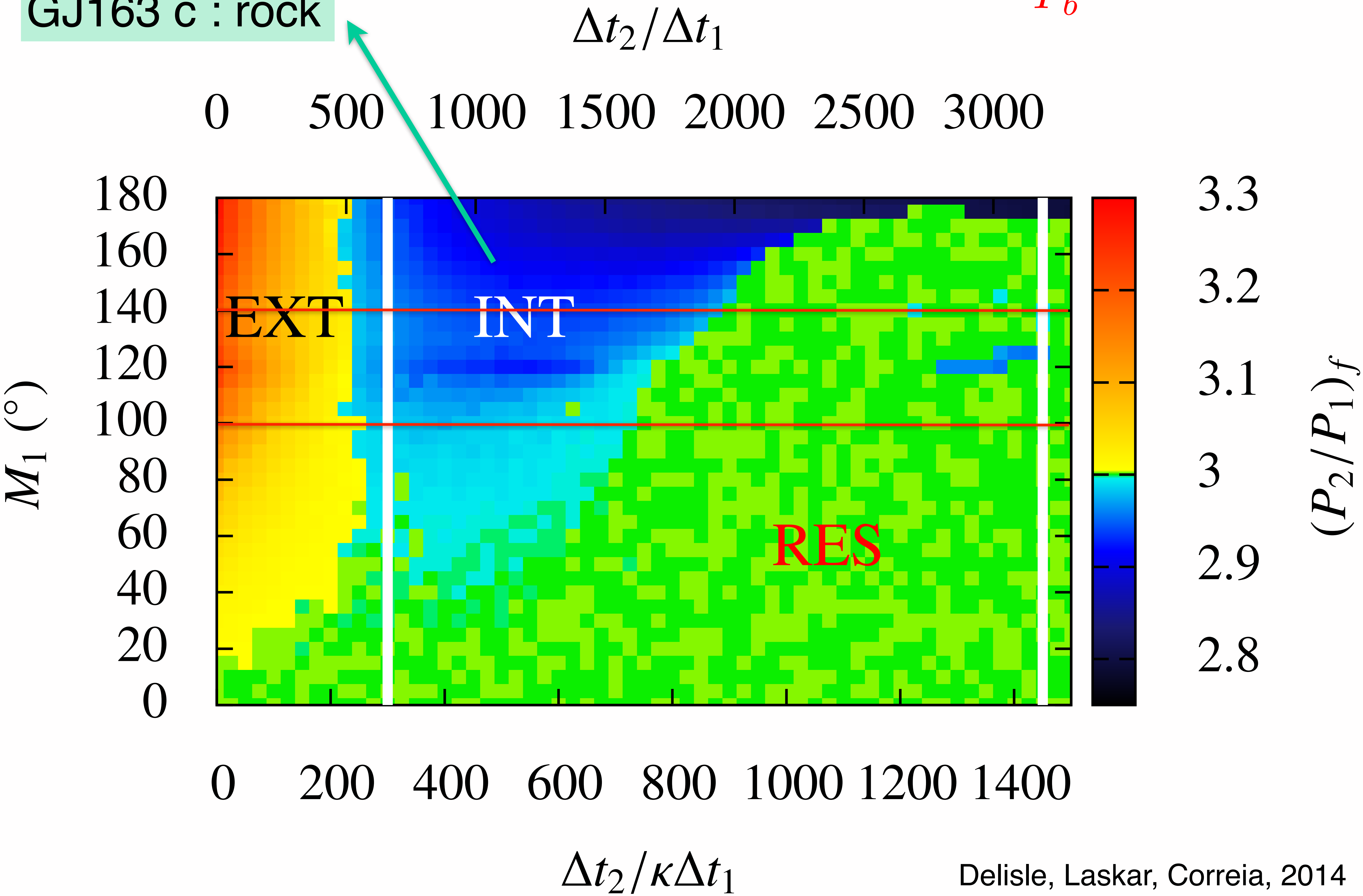

Delisle, Laskar, Correia, 2014

Dissipative case: simulation

- Convergent migration (gray dots)
- Locking into 3 : 2 MMR
- Tidal damping (black dots)

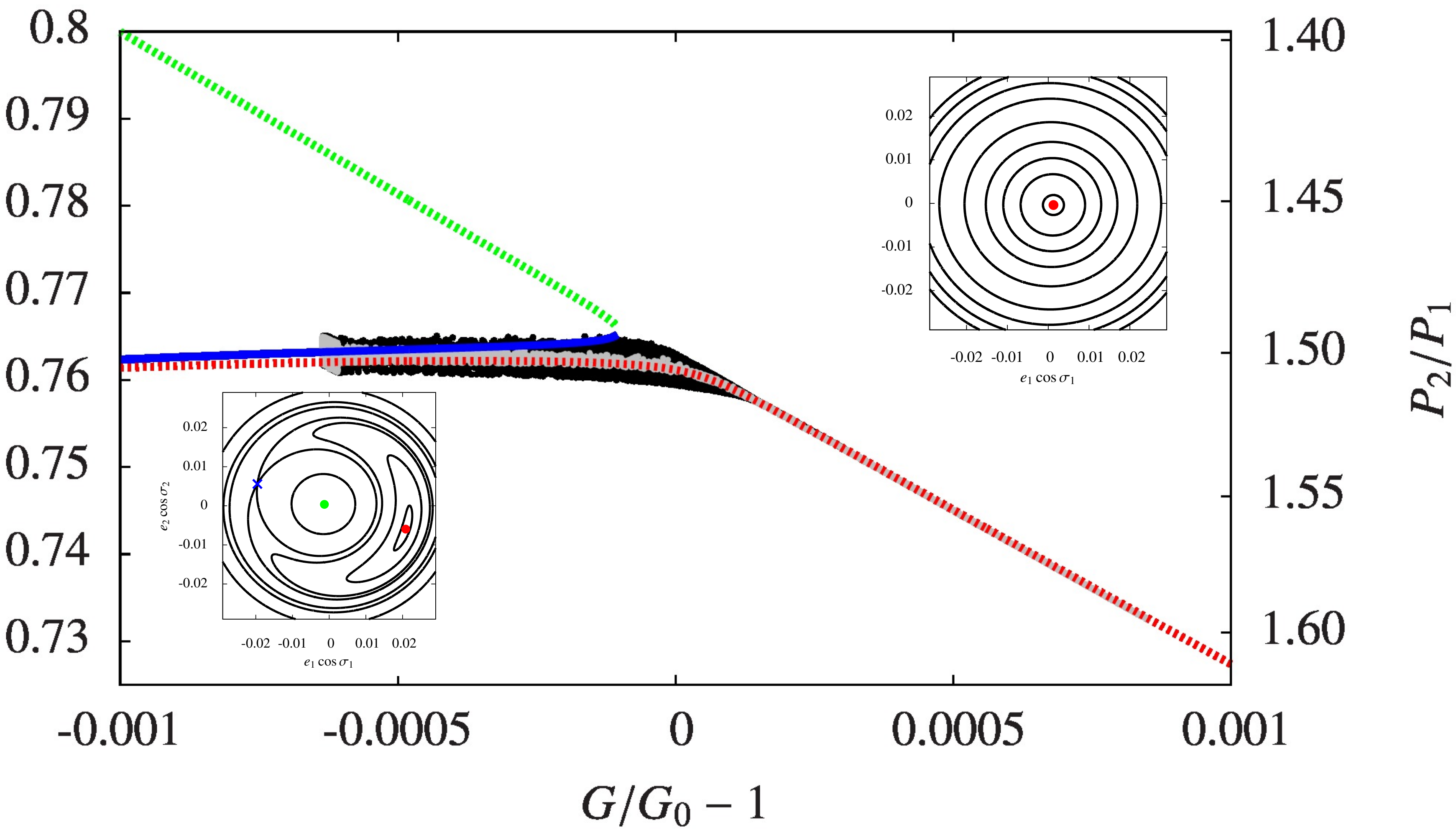

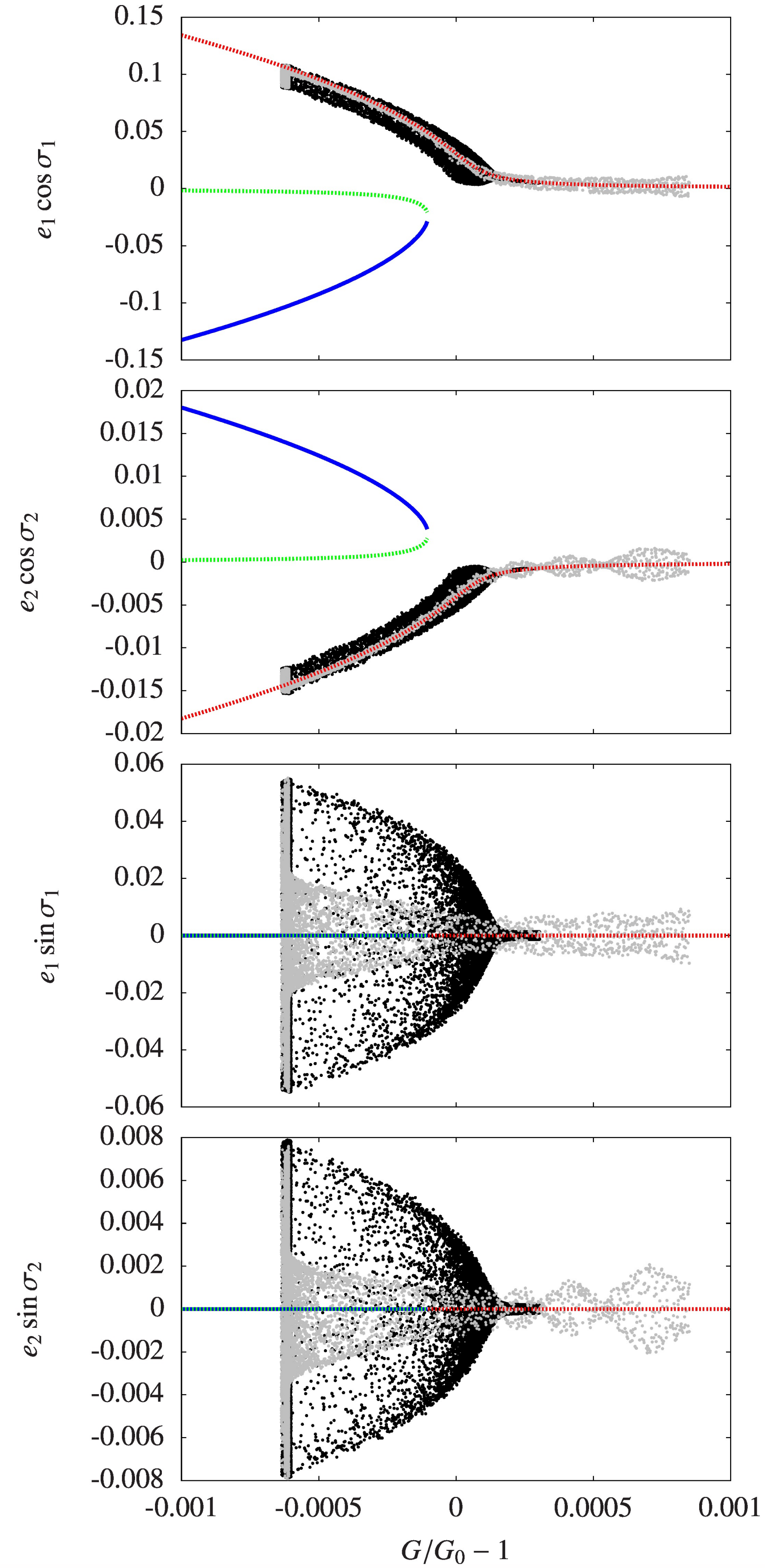

(Delisle, Laskar, Correia, Boué, 2012)

THE ASTROPHYSICAL JOURNAL, 774:52 (8pp), 2013 September 1 doi:10.1088/0004-637X/

ARE THE *KEPLER* NEAR-RESONANCE PLANET PAIRS DUE TO TIDAL DISSIPATION?

MAN HOI LEE[1], D. FABRYCKY[2,3,5], AND D. N. C. LIN[3,4]
[1] Department of Earth Sciences and Department of Physics, The University of Hong Kong, Pokfulam Road, Hong Kong; mhlee@hku.hk
[2] Department of Astronomy and Astrophysics, University of Chicago, 5640 S. Ellis Ave., Chicago, IL 60637, USA; daniel.fabrycky@gmail.com
[3] UCO/Lick Observatory, University of California, Santa Cruz, CA 95064, USA; lin@ucolick.org
[4] Kavli Institute for Astronomy and Astrophysics and School of Physics, Peking University, China
Received 2013 April 11; accepted 2013 July 18; published 2013 August 16

ABSTRACT

The multiple-planet systems discovered by the *Kepler* mission show an excess of planet pairs with period ratios just wide of exact commensurability for first-order resonances like 2:1 and 3:2. In principle, these planet pairs could have both resonance angles associated with the resonance librating if the orbital eccentricities are sufficiently small, because the width of first-order resonances diverges in the limit of vanishingly small eccentricity. We consider a widely held scenario in which pairs of planets were captured into first-order resonances by migration due to planet–disk interactions, and subsequently became detached from the resonances, due to tidal dissipation in the planets. In the context of this scenario, we find a constraint on the ratio of the planet's tidal dissipation function and Love number that implies that some of the *Kepler* planets are likely solid. However, tides are not strong enough to move many of the planet pairs to the observed separations, suggesting that additional dissipative processes are at play.

Key words: celestial mechanics – planetary systems – planets and satellites: general

Lee, Fabrycky, Lin, 2013

$$t/T_1 > 50 - 1000$$

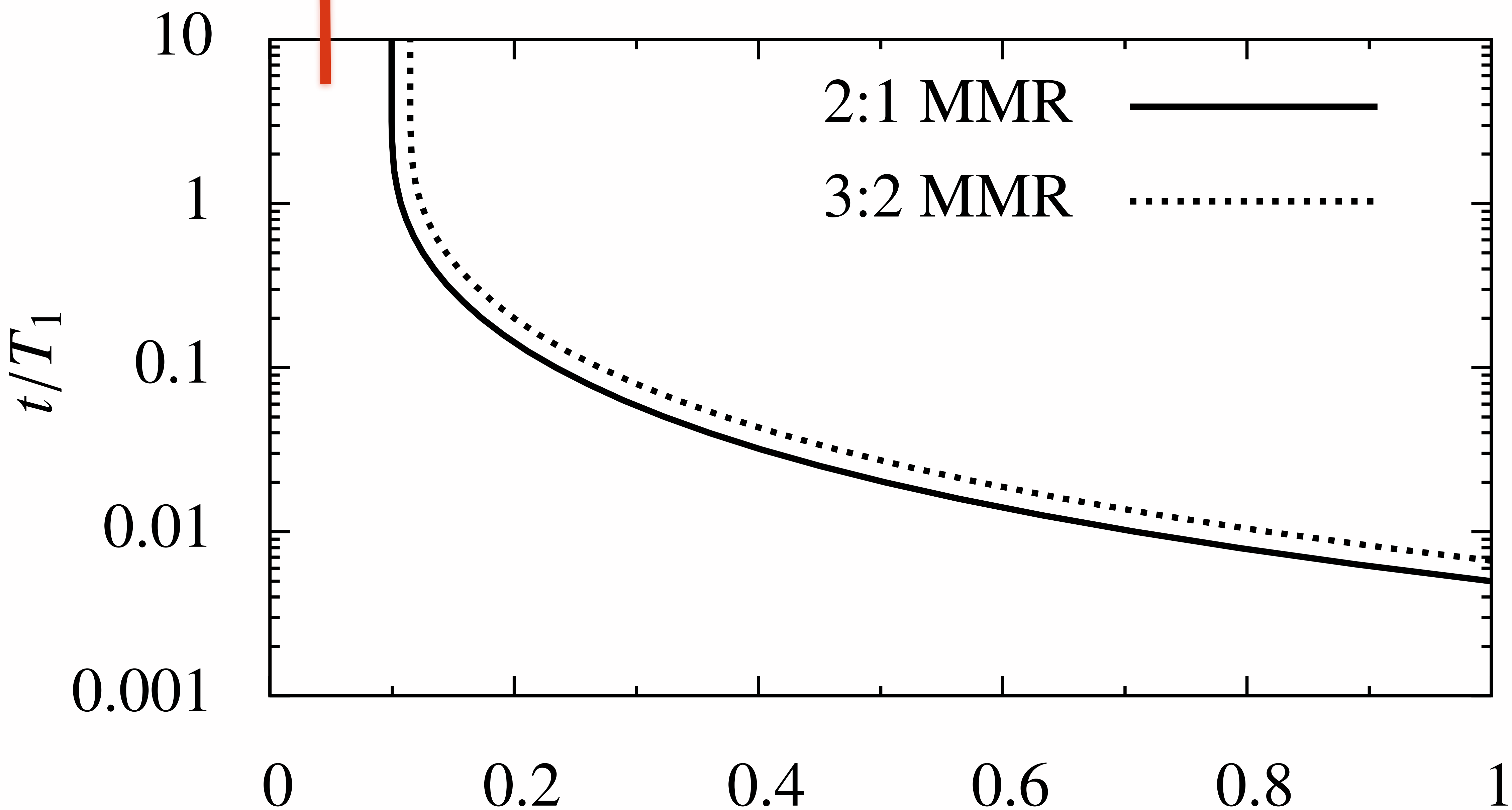

Eccentricity when leaving the resonance $e_{1,0}$

Delisle, Laskar, Correia, 2014

Tidal origine ?

resonant systems

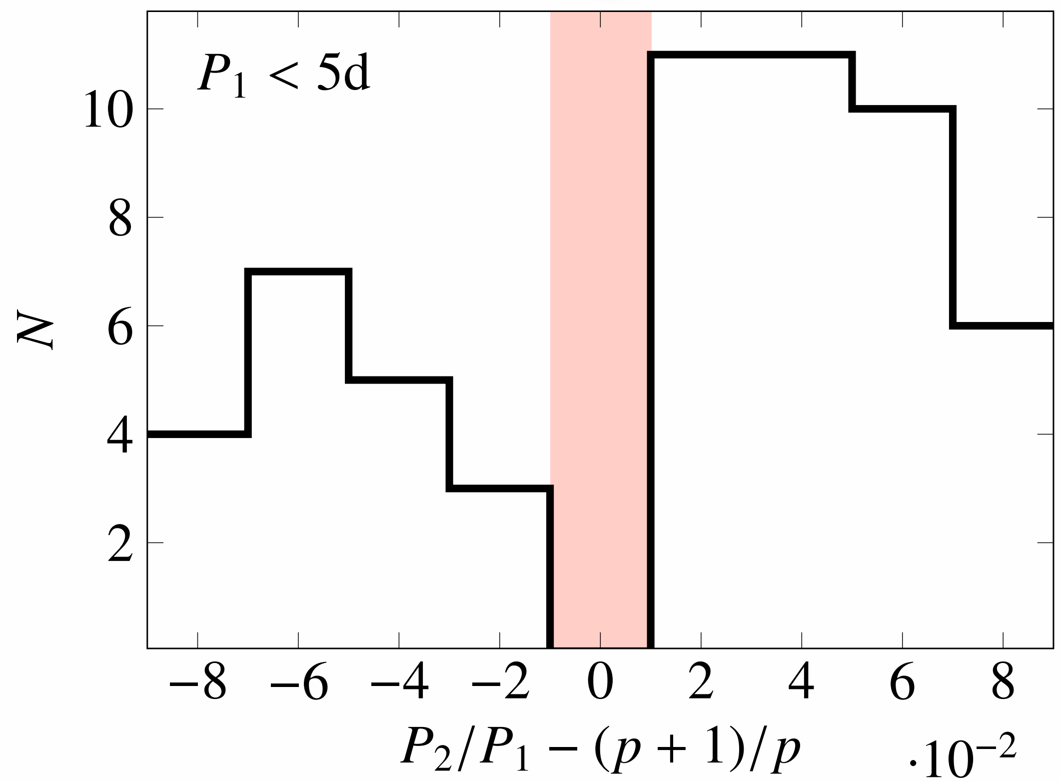

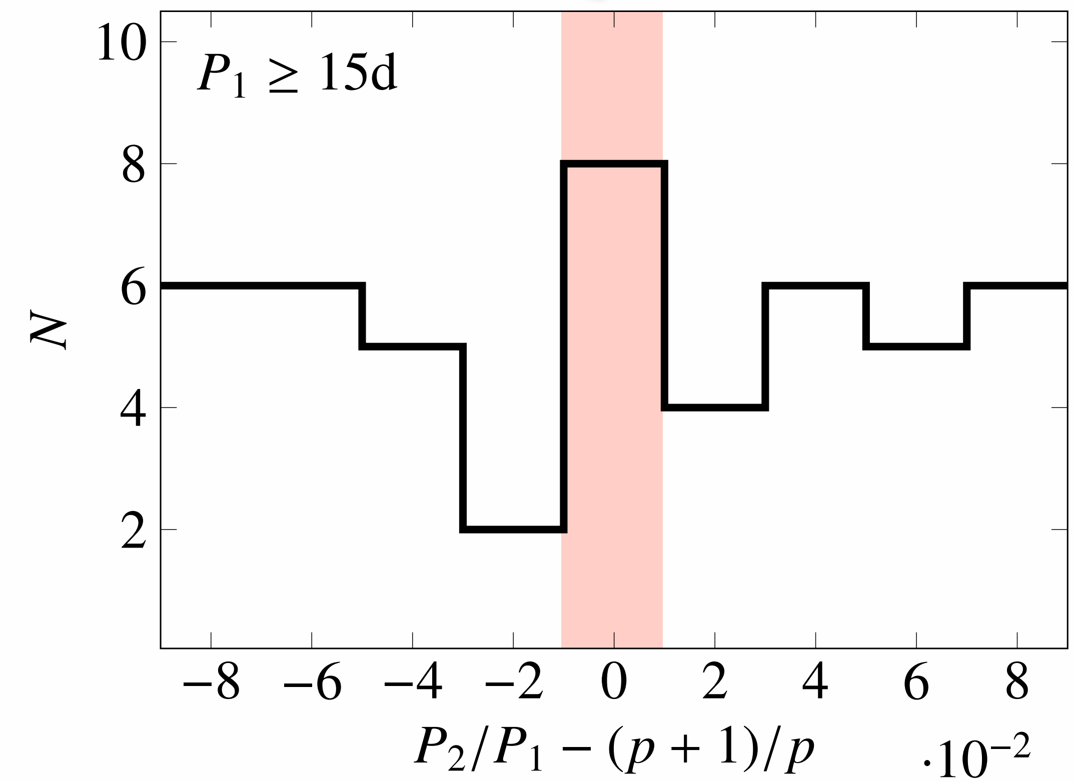

dependence of semi major axis

Delisle & Laskar, 2014

Tidal origine ?

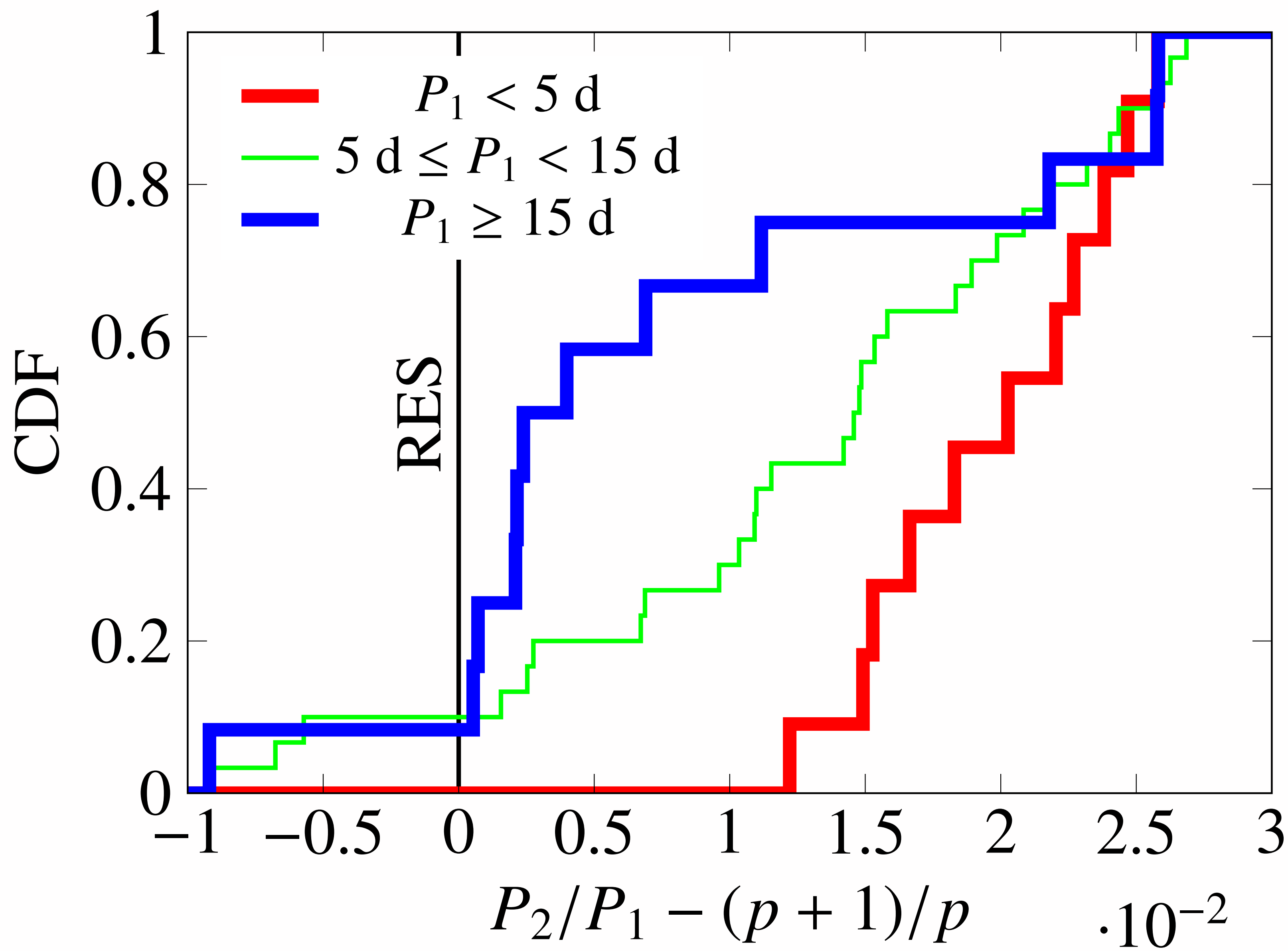

dependence of semi major axis

Delisle & Laskar, 2014